Dalton Transactions

ROYAL SOCIETY OF CHEMISTRY

PERSPECTIVE

View Article Online
View Journal | View Issue

Cite this: *Dalton Trans.*, 2024, **53**, 2413

Coordination-induced bond weakening and small molecule activation by low-valent titanium complexes

Ugochinyere N. Oloyede and Robert A. Flowers, II *

Bond activation of small molecules through coordination to low valent metal complexes in M···X–H type interactions (where X = O, N, B, Si, *etc.*) leads to the formation of unusually weak X–H bonds and provides a powerful approach for the synthesis of target compounds under very mild conditions. Coordination of small molecules like water, amides, silanes, boranes, and dinitrogen to Ti(III) or Ti(II) complexes results in the synergetic redistribution of electrons between the metal orbitals and the ligand orbitals which weakens and enables the facile cleavage of the X–H or N–N bonds of the ligands. This review presents an overview of coordination-induced bond activation of small molecules by low valent titanium complexes. In particular, the applications of low valent titanium-induced bond weakening in nitrogen fixation are presented. The review concludes with potential future directions for work in this area including low-valent Ti-based PCET systems, photocatalytic nitrogen reduction, and approaches to tailoring complexes for optimal bond activation.

Received 17th October 2023,
Accepted 19th December 2023

DOI: 10.1039/d3dt03454b

rsc.li/dalton

1. Introduction

1.1. Background

Titanium, the ninth most abundant element and the second most abundant transition metal in the Earth's crust, is the first member of the 3d transition series with four valence elec-

Department of Chemistry, Lehigh University, Bethlehem, Pennsylvania 18015, USA. E-mail: rof2@lehigh.edu

Ugochinyere N. Oloyede

Ugochinyere Nancy Oloyede was born in Lagos, Nigeria and received her bachelor's and master's degrees in industrial chemistry from the University of Ibadan (UI). During her master's program at UI, she conducted research with Professor Folasegun Dawodu on the thermodynamic and kinetic studies of low-cost adsorbents for crude oil spillage remediation. She is currently a graduate student in the Flowers group at Lehigh University. Her research focuses on developing and studying low-valent catalytic titanocene-mediated systems for chemical synthesis.

Robert A. Flowers

Robert A. Flowers II received his B.S. from East Stroudsburg University in 1986 and his Ph.D. from Lehigh University in 1991. He was a postdoctoral fellow in the Laboratory of Ned Arnett at Duke University from 1991 to 1994. After starting his career at the University of Toledo and moving to Texas Tech University, he was recruited to Lehigh University in 2004 and was appointed the Danser Distinguished Faculty Chair in Chemistry in 2008. He is currently the Herbert J. and Ann L. Siegel Dean of the College of Arts and Sciences. His research focuses on the mechanistic studies of single electron and proton-coupled electron transfer from low-valent rare earth and early transition metal reagents.

trons, [Ar] $3d^2$ $4s^2$.[1] TiO_2, a byproduct of most Ti-catalyzed reaction work-ups, is generally non-toxic unlike other metals such as Ni, Pt, and Au.[2] The readily accessible and environmentally-friendly properties of titanium make it an attractive metal in the design of organometallic complexes for the mediation of organic transformations. The facile transition of Ti-based complexes between the Ti(II), Ti(III) and Ti(IV) oxidation states has enabled accessibility to various mechanistic paradigms in redox chemistry.[3–7]

Among the reactions that employ the Ti(III)–Ti(IV) redox couple are the reduction and cyclization of epoxides,[8] Barbier-type reactions,[9] intermolecular couplings,[10] and synthesis of stereo-controlled compounds.[11] A notable and recent example of a Ti(III)-mediated redox transformation is the photocatalytic reduction of epoxides. In this work, Gansäuer and Flowers demonstrated that excitation of titanocene dichloride, $(\eta^5\text{-}C_5H_5)_2TiCl_2$, with green light in the presence of an amine generates the active $(\eta^5\text{-}C_5H_5)_2TiCl$ intermediate that facilitates the reduction of epoxides, hence discarding the need for stoichiometric metal reductants (Scheme 1).[12]

Ti(II) or lower valent titanium (LVT) is another accessible oxidation state and has an important place in synthetic chemistry. Ti(II) complexes have been implicated in transformations such as the McMurry-type C–C coupling reactions,[7,13,14] intramolecular cyclization,[15,16] pinacol coupling,[17] and N-heterocycles synthesis *via* dinitrogen fixation.[18] The active Ti(II) species have strong reducing and coordinating character and are usually prepared by treating high valent Ti-halides or $Ti(O^iPr)_4$ with reducing agents (such as Li, Mg, or Grignard reagents).[19] Vol'pin and Shur reported the reduction of dinitrogen to ammonia using LVT.[20,21] The scheme below shows the cyclization of (silyloxy)enyne mediated by Ti(II) in the total synthesis of (−)-7-demethylpiericidin A_1 (Scheme 2).[15] The redox chemistry of titanium complexes is extensive and several comprehensive reviews have been published by Schafer,[22] Zhu,[23] and McCallum.[5]

1.2. Chemistry of titanium-induced bond activation

Titanium can exist in various oxidation states including Ti(II), Ti(III), and Ti(IV) of which Ti(IV) is the most stable. Ti(IV) possesses empty d-orbitals allowing it to act as a Lewis acid to form coordinate bonds with electron donating ligands. The presence of an unoccupied d-orbital in Ti(IV) makes it highly favorable for coordination with diverse electron-donating species and enhances its reactivity to engage in a variety of chemical reactions. Ti(III) and Ti(II) also exhibit Lewis acidity, although not as pronounced as Ti(IV), due to the presence of partially-filled d-orbitals. The Lewis acid behavior and reactivity of Ti(III) and Ti(II) can be influenced by several factors including the redox environment, the nature of ligands, and the steric hindrance of the complex.[13,14] Coordination of small molecules to low valent titanium in an M–X–H or M → N_2 type

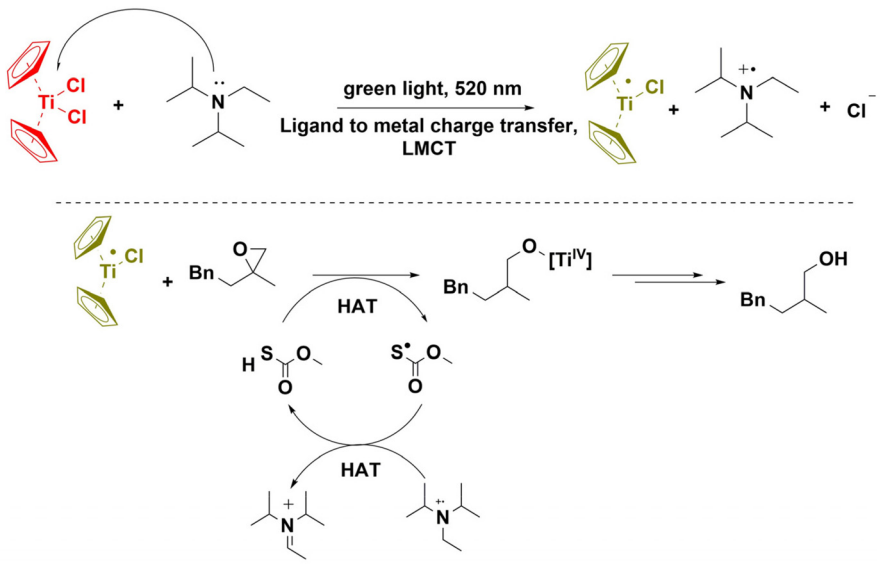

Scheme 1 Photocatalytic Ti(III)-mediated reduction of epoxide. Reproduced from ref. 12. Copyright 2020 Wiley-VCH Verlag GmbH & Co. KGaA.

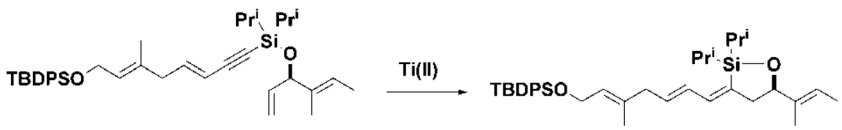

Scheme 2 Ti(II)-mediated cyclization of (silyloxy)enyne. Reproduced with permission from ref. 15. Copyright 2006 American Chemical Society.

bond (where M = metal and X = heteroatom) can result in bond activation or bond weakening of the X–H bond or the triple bond of the coordinated dinitrogen. The M → N_2 type bond activation interaction is rationalized using the Dewar–Chatt–Duncanson bonding model. Dewar, Chatt and Duncanson proposed that the bond between a transition metal and a ligand (unsaturated) had two synergistic components: donation of the electron density from the π-bond of the ligand to a suitable vacant hybrid orbital on the metal and back-donation from the filled metal d orbitals to the empty π* orbital of the ligand.[24,25] For early transition metals like titanium, the interaction involves ligand-to-metal σ or π bonding and metal dπ back-donation. The back-donation synergy results in the redistribution of the electron density, thereby decreasing the overall stability and strength of the N–N triple bond (Fig. 1).

For M–X–H type bond activation, the bond weakening observed in the associated X–H bond is rationalized by the formation of a thermodynamically favored product occurring through formal H-atom transfer from the complex.[26] Such interactions result in proton-coupled electron transfer (PCET) processes in chemical reactions. The activation of strong bonds through coordination provides access to reactions that otherwise would be challenging and a number of synthetically important reactions have been developed using this approach.[27] PCET plays a key role in fundamentally important transformations in both industrial and biological processes[28] and avoids the necessity of large overpotentials as well as high energy intermediates.[29] Unlike in hydrogen atom transfer (HAT) reactions where the protons and electrons are transferred between the same donor and acceptor, in PCET reactions, the transfer of protons and electrons occurs between different centers.[26,30] The thermochemistry of the process of H-atom loss from the M–X–H type interaction is governed by $E°$ at the metal center and the pK_a values of the oxidized and reduced species in solution (see Fig. 2).[26,31,32] As a consequence, the bond dissociation free energy (BDFE) can be calculated using the Bordwell thermodynamic equation (see below), where C_G is a solvent dependent thermodynamic constant that accounts for the energy required to form a hydrogen atom from a proton and an electron. Hence, the strength of the X–H bond in the ligand is attenuated by the strength of the reductant L_nM–X–H and the acid L_nM^+–X–H (see Fig. 2)

$$\mathrm{BDFE} = 1.37\mathrm{p}K_a + 23.06E° + C_G. \quad (1)$$

This straightforward, but powerful approach enables the prediction of the degree of change in bond strength that occurs through coordination-induced bond weakening and therefore can be used to predict the limits and thermodynamic feasibility of reactions. In this review, reports of bond activation facilitated by low-valent titanium-based compounds will be discussed. Applications of bond-weakening in synthesis facilitated through coordination to a titanium metal center will be detailed with a focus on the reduction of dinitrogen and other nitrogen-containing compounds.

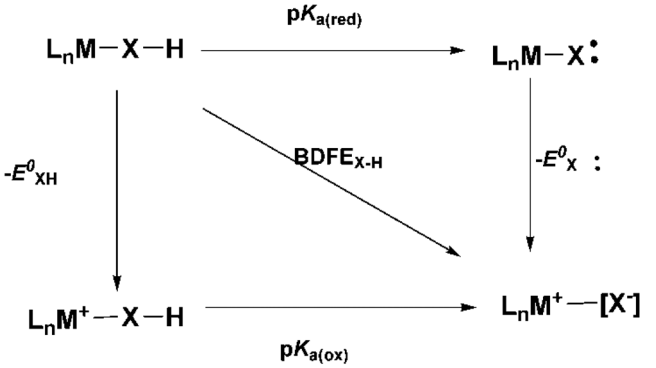

Fig. 2 Bordwell thermodynamic cycle. Reproduced with permission from ref. 26. Copyright 2021 American Chemical Society.

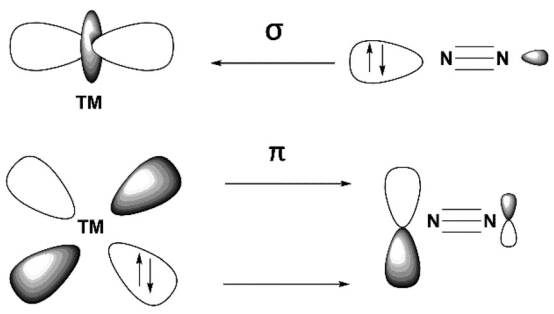

Fig. 1 The Dewar–Chatt–Duncanson model for transition metal (TM)-dinitrogen bonding.

2. Heteroatom–hydrogen bond activation through coordination to low-valent titanium

2.1. Water

The activation of small molecules such as water, methanol, and amines through coordination to a low-valent metal center is a promising way to provide a sustainable route for the synthesis of organic compounds and the production of "green" fuels. The classic example of this phenomenon is the significant bond weakening observed in the O–H bond of water (approximately 60 kcal mol^{-1}) resulting from coordination to low-valent titanocene.[33–35] In 2010, Cuerva and coworkers demonstrated that water and amines can disrupt the dimeric structure formed by titanocene dichloride in the low valent form, $((\eta^5\text{-}C_5H_5)_2TiCl)_2$, and coordinate to the titanium metal center (see Table 1). This interaction weakens the X–H bond to facilitate the reduction of the substrate *via* a carbon-centered radical intermediate.[34]

Theoretical calculations showed the highest bond weakening in water (Δ(BDE) = 58.6 kcal mol^{-1}) and the least bond weakening in the secondary amine (Δ(BDE) = 19.1 kcal mol^{-1}). The higher ΔBDE observed in the oxygen containing molecules

Table 1 Summary of the bond dissociation energies (BDEs) of the X–H bond in small molecules bound to Ti(III)

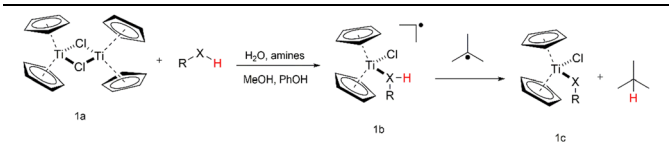

RX-H	BDE, kcal mol^{-1}	$(\eta^5\text{-}C_5H_5)_2TiCl$ (RX-H)	BDE, kcal mol^{-1}	Δ(BDE), kcal mol^{-1}
HO-H	108.1	HO-H	49.4	58.6
DO-D	110.3	DO-D	51.4	58.8
MeO-H	93.5	MeO-H	42.6	50.9
PhO-H	74.3	PhO-H	39.6	34.7
NH_2-H	100.4	NH_2-H	65.0	35.4
$MeNH_2$-H	92.4	$MeNH_2$-H	63.7	28.7
Me_2N-H	86.7	Me_2N-H	67.6	19.1

Reproduced with permission from ref. 34. Copyright 2010 American Chemical Society.

is likely attributed to the high oxophilicity of titanium. The stronger the coordination of the heteroatom to the metal, the greater the bond weakening of the associated X–H bond.[36] A number of intermediates were proposed for modes of water complexation to titanocene as shown below in Fig. 3.[35] Using EPR spectroscopy, cyclic voltammetry (CV) and computational methods, Gansäuer and coworkers were able to establish that **1b** is absent in zinc reduced THF solutions of $(\eta^5\text{-}C_5H_5)_2TiCl_2$ and H_2O.[35]

EPR studies of a Zn-$(\eta^5\text{-}C_5H_5)_2TiCl_2$ THF solution with or without water revealed that the unpaired electron resides in a $3d_{z^2}$ orbital of the low valent titanocene. However, there were

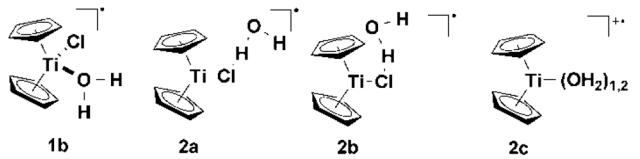

Fig. 3 Modes of water coordination of low-valent titanocene. Reproduced with permission from ref. 35. Copyright 2012 Wiley-VCH Verlag GmbH & Co. KGaA, Weinheim.

significant changes to the g_x value with increasing amounts of water under experimental conditions. Also, CV studies revealed the presence of the cationic intermediate $[Cp_2Ti]^+$ when water is added to a Zn-reduced THF solution of $(\eta^5\text{-}C_5H_5)_2TiCl_2$. The addition of HMPA (HMPA = hexamethyl phosphoramide) rather than water to a Zn-reduced THF solution of $(\eta^5\text{-}C_5H_5)_2TiCl_2$ did not generate solvated $[Cp_2Ti]^+$ indicating that chloride ion solvation through hydrogen bonding by water is necessary for the formation of $[Cp_2Ti]^+$. The addition of 10 equivalents of water generated the species $[Cp_2Ti(OH_2)]^+$ while the addition of higher water equivalents (>100 equiv.) resulted in the coordination of another water molecule to the Ti-center to form $[Cp_2Ti(OH_2)_2]^+$. Computational studies showed that the complexation of THF molecules to the coordinated water leads to substantial stabilization of the cationic species $[Cp_2Ti]^+$. Coordination of one H_2O*2THF to the Ti-center of $[Cp_2Ti]^+$ is more favorable by about −41 kcal mol^{-1} while the complexation of an additional H_2O*2THF further stabilizes the intermediate $[Cp_2Ti(OH_2$*2THF$)]^+$ by about −20 kcal mol^{-1}. The scheme below illustrates the findings of these studies (Scheme 3).

Another important discovery from this work is the role of the solvent in attenuating the reactivity of water-solvated titanocene. Although the O–H BDE of **2e** is lower than those of other formal HAT donors including stannanes,[37,38] reactions of **2e** with alkyl radicals are slower and a result of unfavorable desolvation of THF. Overall, these studies demonstrate the complexity of metal-water coordinated structures and solvents in these systems, and these variables should be kept in mind when considering rate-limiting structures likely important in similar systems.[39–41]

2.2. Amides

Activation of amide N–H bonds by coordination to a Ti^{III} center has also been reported.[42,43] Knowles and coworkers employed coordination-induced bond weakening to develop a novel free-radical cyclization. The N–H bond of aryl amides with $BDFE_{N-H}$ of approximately 100 kcal mol^{-1} (ref. 44) were weakened by about 33 kcal mol^{-1} by coordination of O to $(\eta^5\text{-}C_5(CH_3)_5)_2TiCl$ (Scheme 4).[42]

The weakened N–H bond enabled TEMPO to function as a formal hydrogen atom acceptor, resulting in the formation of

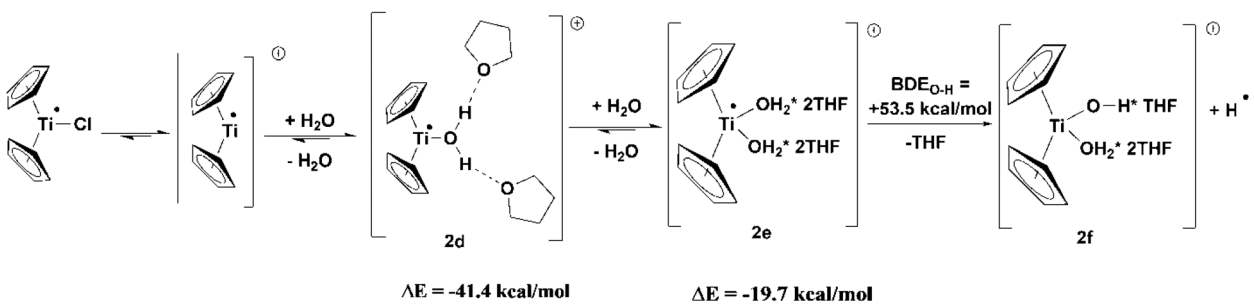

Scheme 3 Water complexation to low-valent titanocene and the stabilizing effect of THF. Reproduced with permission from ref. 35. Copyright 2012 Wiley-VCH Verlag GmbH & Co. KGaA, Weinheim.

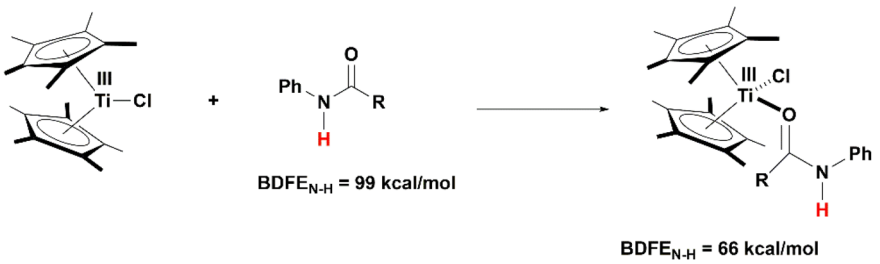

Scheme 4 Bond weakening of the N–H bond of free amide induced by coordination to low-valent Ti. Reproduced with permission from ref. 42. Copyright 2015 American Chemical Society.

a metalated Ti(IV) aza-enolate intermediate which served as a nucleophile in the C–N bond formation (Scheme 5).

Low valent titanocene dichloride, $(\eta^5\text{-}C_5H_5)_2TiCl$, is known to react with TEMPO to form an isolable Ti^{IV} complex with a relatively weak Ti–O bond of about 67 kcal mol^{-1}.[45] The strengths of the Ti–O bond in titanocene-TEMPO complexes were found to depend "sensitively" on the ancillary ligation at titanium. The more ligated the titanium center, the longer the Ti–O bond distance and in-turn, the weaker the Ti–O bond.[46,47] The additional methyl substituents on the cyclopentadienyl rings of titanocene dichloride, significantly weakened the Ti–O bond to ~2 kcal mol^{-1}, thereby making titanocene–TEMPO interactions thermodynamically unfavorable and allowing the coordination of amide substrates to the metal center. Representative examples demonstrating the scope of the reaction are shown below in Table 2.

Similarly, Gansäuer and coworkers developed a titanocene–amide catalyst (**3**) which exists as three different species in the Zn-reduced form (**3**, **3a**, and **3b**). The intermediates enabled the coordination of the pendant amide to the low-valent Ti making the N–H bond a good formal hydrogen atom donor. The unique feature of this work is that not only is titanium being used as a reductant for the substrate, but also to form a formal HAT reagent with the pendant amide (see Scheme 6).[48]

DFT calculations revealed that the bond dissociation energy (BDE) of the N–H bond of the amide in complex **3a** is 39 kcal

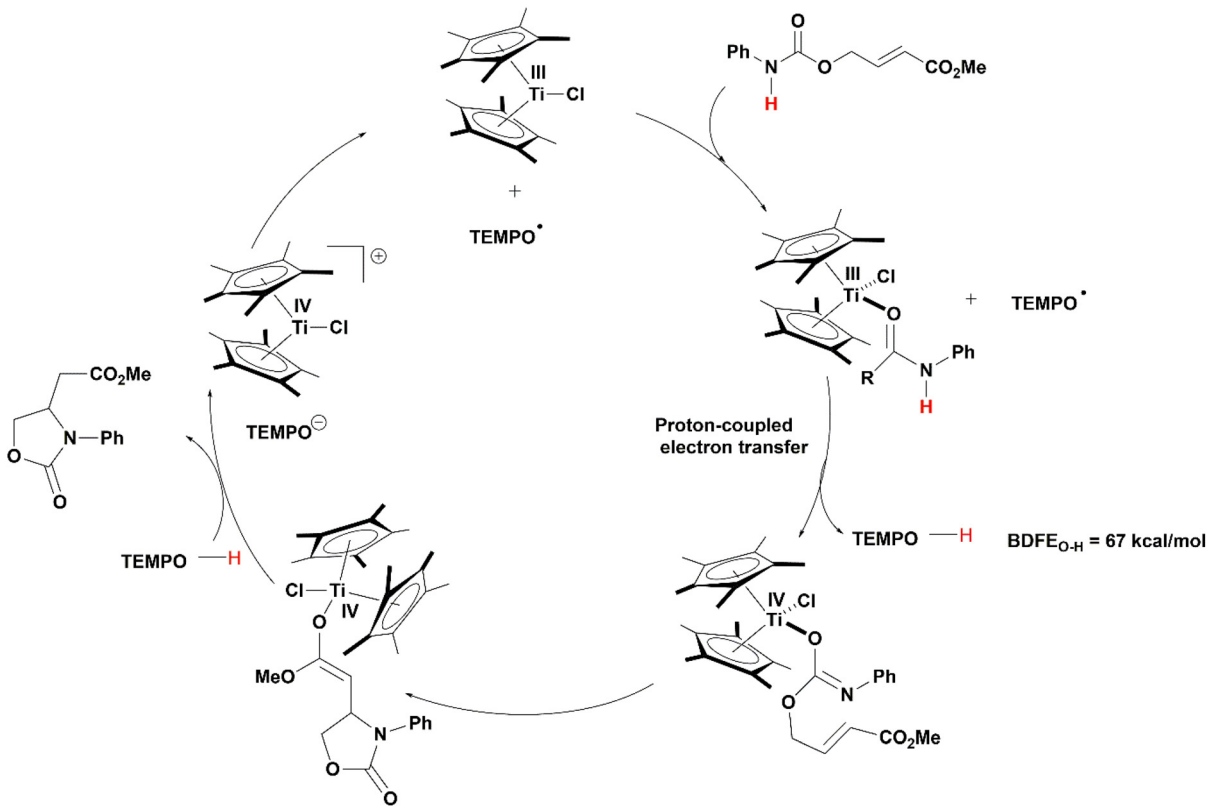

Scheme 5 Catalytic cycle for the free-radical cyclization of amides. Reproduced with permission from ref. 42. Copyright 2015 American Chemical Society.

Table 2 Scope of the free-radical cyclization mediated by low-valent titanocene

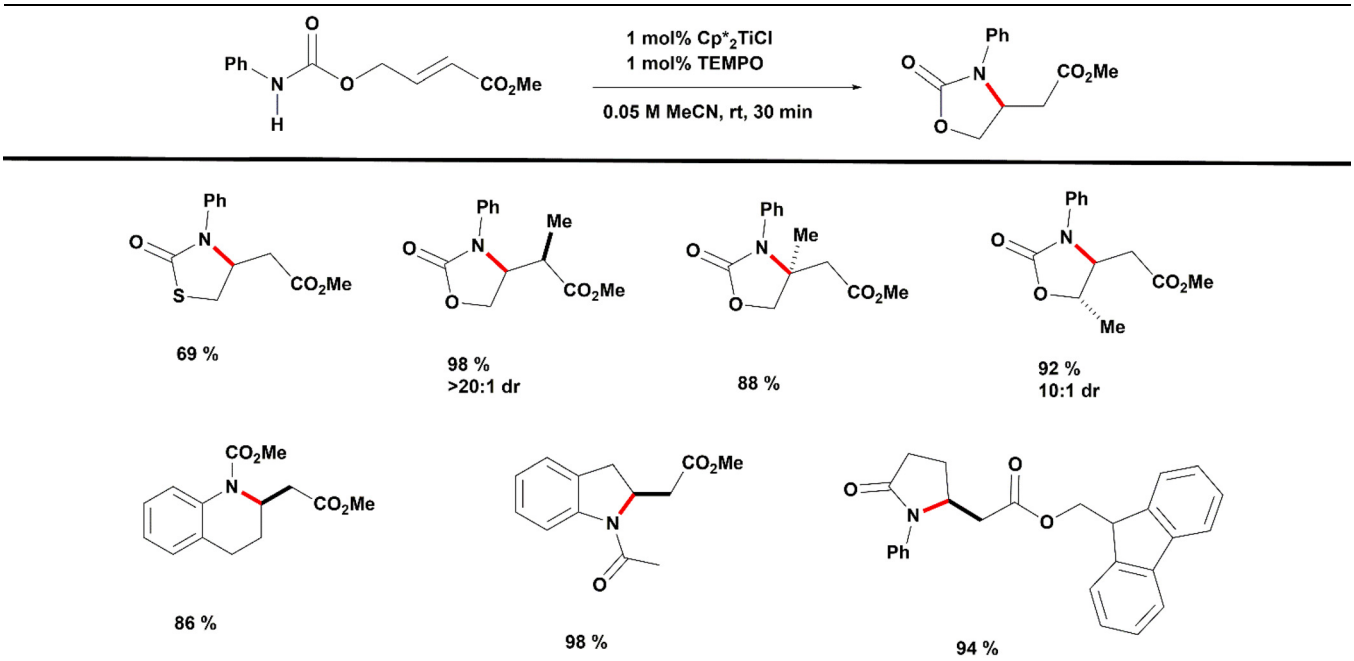

Reproduced with permission from ref. 42. Copyright 2015 American Chemical Society.

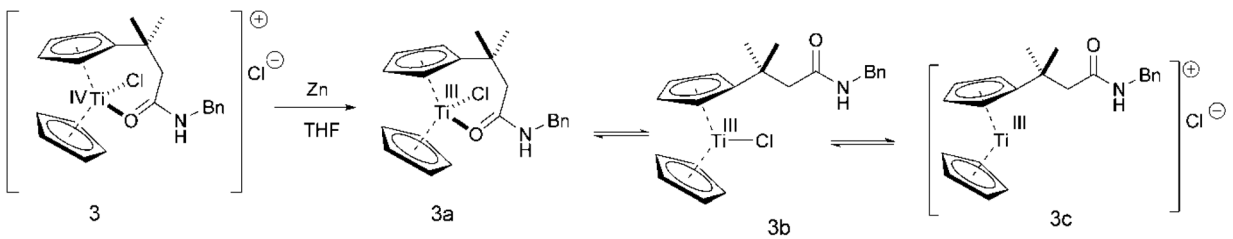

Scheme 6 Zn-reduced titanocene–amide complex intermediates found in solution. Reproduced with permission from ref. 48. Copyright 2016 Wiley-VCH Verlag GmbH & Co. KGaA, Weinheim.

mol^{-1} weaker than that of a free amide N–H bond; a consequence of coordination-induced bond weakening. The presence of Zn-reduced species in solutions allows for bifunctional catalysis in epoxide ring opening reactions. In the epoxide ring-opening reduction reaction mechanism, **3b** coordinates to the oxygen of the epoxide to facilitate electron transfer and ring opening reactions while **3a** catalyzes hydrogen atom transfer (HAT) reactions for epoxide reduction (see Scheme 7).

Complex **3** was modified for enantioselective catalysis by adding a methyl substituent to the cyclopentadienyl ring of the titanocene–amide and changing the benzyl substituent on the amide nitrogen. Enantioselectivity in ring opening was observed in the different complexes (**4a–4d**) with **4b** given the most selectivity of 91 : 9 in toluene. Cooperative catalysis with **3a** and Wilkinson's catalyst [Rh(PPh$_3$)$_3$Cl] or Crabtree's catalyst [Ir(cod)PyPCy$_3$]PF$_6$ was employed to effect a more active and selective catalytic system. Wilkinson's catalyst[49] and Crabtree's catalyst[50] are catalysts used for the hydrogenation of olefins in the presence of dihydrogen gas *via* the formation of the active hydride complexes (Scheme 8).

By exploiting the weak N–H bond of the titanocene–amide complex, **4b**, hydrogen atoms were transferred to the transition metal catalysts leading to the formation of the corresponding reactive hydride complexes with significant acceleration in the formation of **4e**. Crabtree's catalyst showed increased reactivity with **4b** at lowered temperatures in toluene with an enantioselectivity of 95 : 5.[48]

2.3. Silanes

The coordination of silanes to a metal center by η^2 σ bonds has been reported to induce bond weakening of the Si–H bond.[51–54] This nonclassical interaction has been studied in both early- and mid-transition metal complexes.[53,54] These complexes exhibit special structural and bonding characteristics attributed to the weak σ Si–H bond and the hypervalency of Si.[55] The basis of the metal–silane interaction is described

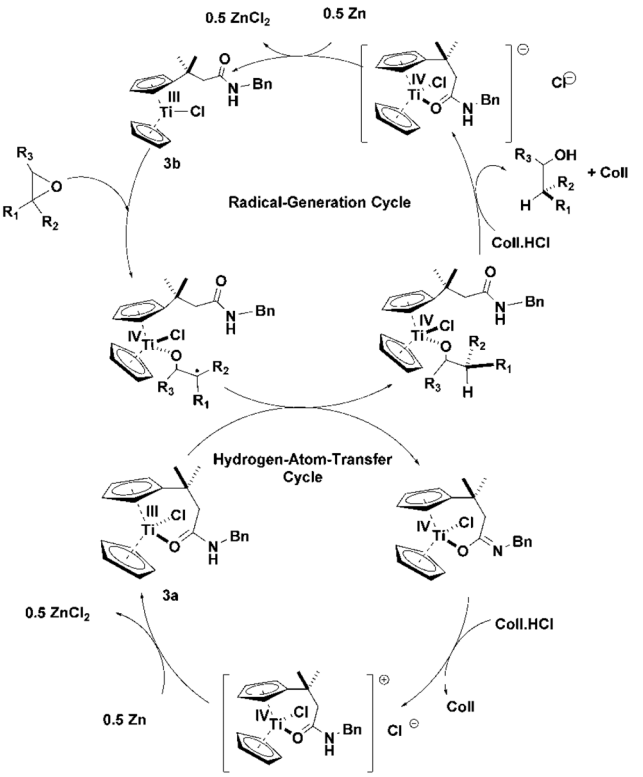

Scheme 7 Titanocene–amide mediated epoxide ring opening. Reproduced with permission from ref. 48. Copyright 2016 Wiley-VCH Verlag GmbH & Co. KGaA, Weinheim.

by the Dewar–Chatt–Duncanson model of ligand-to-metal σ bonding and metal dπ back-donation (see Fig. 4).

Bent organosilicon metallocenes of group 4 metals have interesting chemistry and are excellent generators of M(II) complexes (M = Ti, Zr, Hf) in reactions involving alkynes under mild conditions.[56–59] A well-known example is the reaction of a

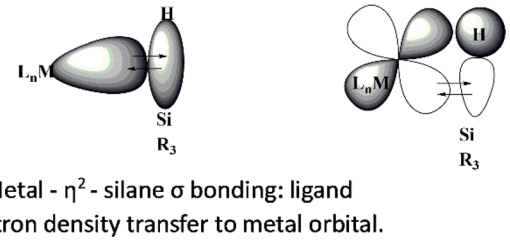

Metal - η² - silane σ bonding: ligand electron density transfer to metal orbital.

Fig. 4 Dewar–Chatt–Duncanson model of metal-silane bonding interaction. Reproduced with permission from ref. 55. Copyright 2002 the Royal Society of Chemistry.

THF solution of titanocene dichloride, $(\eta^5\text{-}C_5H_5)_2TiCl_2$ with magnesium in the presence of (3,3-dimethylbut-1-yn-1-yl)trimethylsilane to generate the Ti(II) complex $Cp_2Ti(\mu^2\text{-}^t BuC_2SiMe_3)$ (**5**) having a titanacyclopropene structure.[53] Complex **5a** can undergo alkyne substitution with (3,3-dimethyl-1-butyn-1-yl)dimethylsilane in *n*-hexane to generate the complex $Cp_2Ti(\mu^2\text{-}^t BuC_2SiHMe_2)$ (**5b**) which was isolated as air- and moisture-sensitive dark red crystals exhibiting temperature-dependent Si–H–Ti interactions (see Scheme 9).

The solid state structure of complex **5b** shows a Ti–H bond distance of 1.82 Å which is within the range of known titanium hydride complexes,[60] a Ti–Si bond distance of 2.655 Å typical of titanocene-silyl complexes, and a Si–H bond length of 1.42 Å which is within the range of tetrahedral silanes.[61] Lin and coworkers further investigated the interactions of the coordinated C–C triple bond and the Si–H bond of the complex **5** by employing *ab initio* calculations with a focus on the structural and electronic effects of the competing metal-acetylene and metal–(H–Si) interactions.[62] The *cis* conformation of the H–Si bond with reference to the acetylene moiety was explained to be a result of the strong σ*-accepting ability of the H–Si bond. This type of interaction has previously been reported to exist in transition metal σ complexes.[54] Theoretical

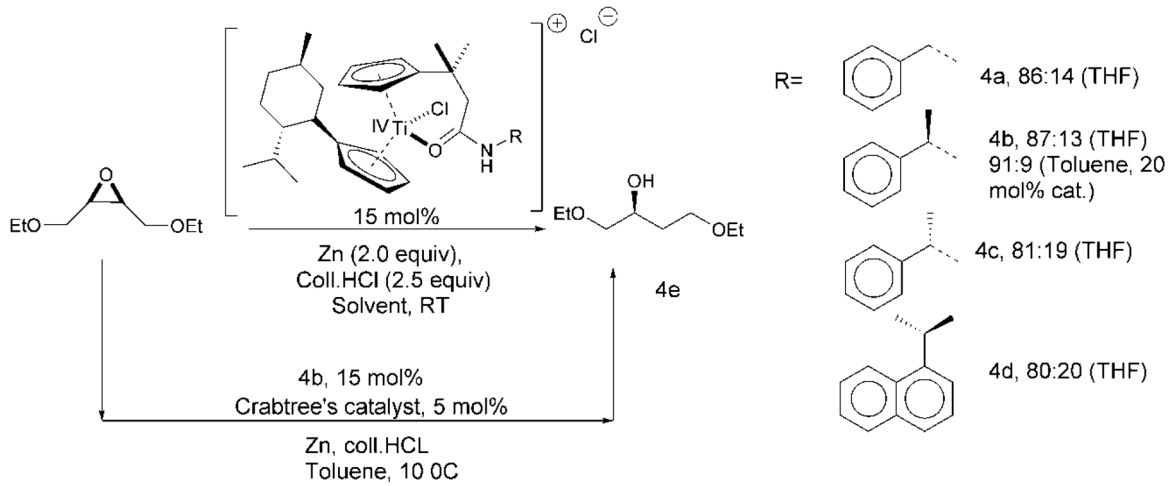

Scheme 8 Menthyl-substituted titanocene–amide cooperative epoxide reduction with Crabtree's catalyst. Reproduced with permission from ref. 48. Copyright 2016 Wiley-VCH Verlag GmbH & Co. KGaA, Weinheim.

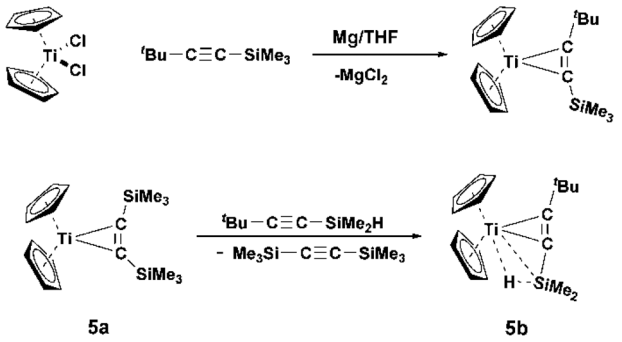

Scheme 9 Synthesis of $Cp_2Ti(\mu^2\text{-}^tBuC_2SiMe_3)$ (**5**). Temperature-dependent Si–H–Ti interaction. Reproduced with permission from ref. 53. Copyright 1995 American Chemical Society.

calculations and a study of the Hartree–Fock valence electron density revealed competing interactions between the C–C triple bond and the H–Si with the titanium center. The presence of the Ti–(H–Si) interaction weakened both the ligand-to-metal σ donation and π-metal-to-ligand back-bonding Ti-acetylene interactions. These findings confirm the strong nature of the Ti–(H–Si) interaction and bond activation.

Scherer and coworkers employed NMR and computational studies to examine the structure–property relationship of several transition metal-silyl complexes and the degree of Si–H bond activation.[63,64] These studies showed that the degree of Si–H activation increases with decreasing magnitude of the J(Si,H) coupling constants and that the negative sign of J(Si,H) validates the presence of a direct Si–H bond (Fig. 5).

It has been reported that electronegative substituents (X) at the silicon atoms in a *trans* position with respect to the bridging η(Si–H) entities enables enhanced M → σ*(H–Si–X) π back-donation that subsequently increases the M–Si bond strength in early transition metal silane complexes.[65] Therefore, to confirm the influence of electronegative substituents on the activation of the Si–H bond by titanium complexes, a series of titanocene-silyl complexes, $Cp_2Ti(PMe_3)(HSiMe_{3-n}Cl_n)$ with n = 1–3, were investigated.

As shown in Table 3, the J(Si,H) coupling constant increased with an increasing number of electronegative substituents. The observed positive sign of J(Si,H) coupling constants in the series is explained by the increasing dominance of the Ti → σ*(H–Si–Cl) π back-donation between the metal and the silane ligand with the increasing number of chlorine substituents at the silicon atom.[63] Overall these studies demonstrate that low valent titanocene can activate the σ Si–H bond through back donation of electrons from the metal orbitals with the degree of Si–H bond activation decreasing with increasing σ Si–H bond strength.

2.4. Boranes

Hartwig and coworkers reported the synthesis of a titanocene-catecholborane complex with unusual coordination of neutral boranes through σ-bonds.[66,67] Treating titanocene dimethyl

Table 3 Electronegative substitutent effect on Si–H bond activation

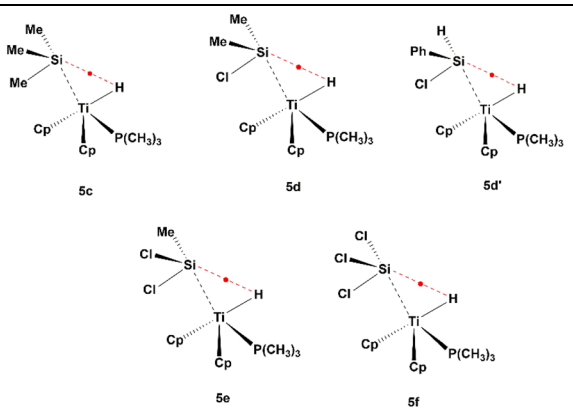

J(Si,H) [Hz]	5c	5d	5d′	5e	5f
$J_{\sigma,\text{total}}$(Si,H)	−67	−58	−50	−64	−65
$J_{\pi,\text{total}}$(Si,H)	+51	+71	+72	+99	+144

Reproduced with permission from ref. 63. Copyright 2016 Wiley-VCH Verlag GmbH & Co. KGaA, Weinheim.

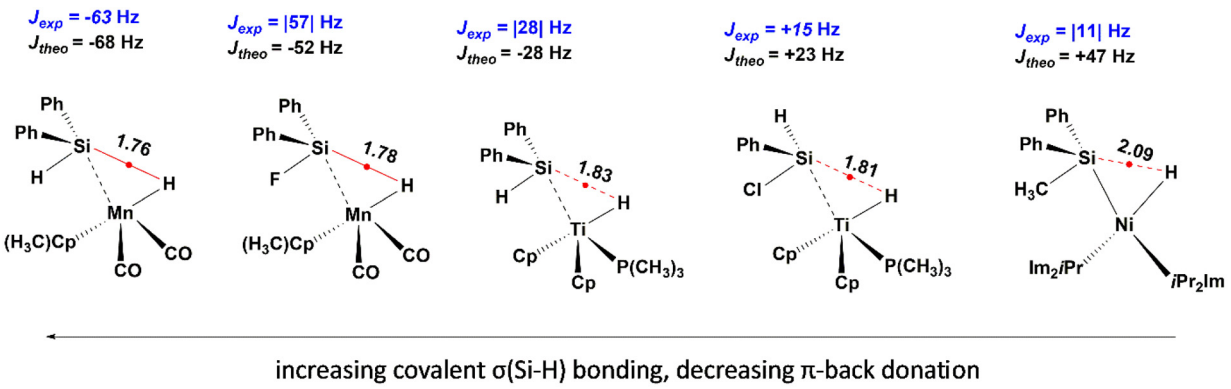

Fig. 5 Si–H bond activation in transition metal complexes. Reproduced with permission from ref. 63 and 64. Copyright 2016 Wiley-VCH Verlag GmbH & Co. KGaA, Weinheim. Copyright 2017 American Chemical Society.

$[(\eta^5\text{-}C_5H_5)_2Ti(CH_3)]_2$ with 3–5 equivalents of catecholborane (HBcat) or 4-(methylcatechol)borane (HBcat′) at −35 °C for 1–2 d precipitated the compounds $Cp_2Ti(HBcat)_2$ (**6**, cat = $O_2C_6H_4$; **7**, 4-MeC_6H_4). Analysis using NMR and IR spectroscopy revealed that both **6** and **7** exist as Ti(II) complexes containing two neutral coordinated boranes. The B–H distance was 1.268 Å, while the Ti–H distance was 1.779 Å, typical of bridging hydrides. The longer Ti–B bond distance of 2.335(5) Å suggests a bond order of less than one and a partially cleaved bond. The observed infrared vibrational frequencies of the hydrides for the complexes **6** and **7** were 1611 and 1680 cm^{-1} which are significantly lower than free catecholborane (ν_{B-H} = 2660 cm^{-1}) consistent with a low B–H bond order. Theoretical calculations demonstrated an interaction which involved B–H σ-bond donation to the metal and a significant back-donation from the metal d orbital into the boron p-orbital (Scheme 10).

Further analysis of the bonding characteristics of the titanocene borane complexes, using $Cp_2Ti[\eta^2\text{-}HB(OH)_2]_2$ and $Cp_2TiPH_3[\eta^2\text{-}HB(OH)_2]$ as model systems, revealed a significant electron density between the two boron atoms and a short B–B distance of 2.194 Å consistent with bonding interactions between the two boron atoms (Fig. 6).[68]

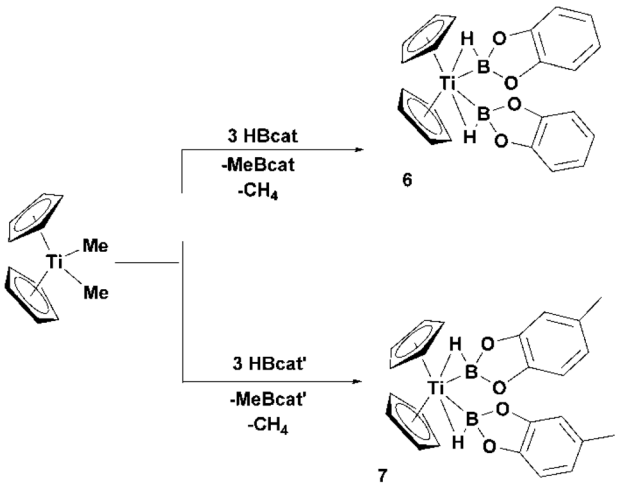

Scheme 10 Coordination of neutral boranes through σ-bonds in the Ti–(B–H) type interaction. Reproduced with permission from ref. 66 and 67. Copyright 1996 and 1999 American Chemical Society.

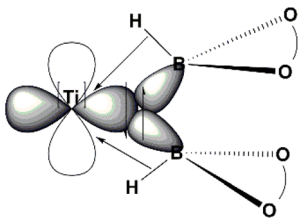

Fig. 6 Orbital representation of the Ti–(B–H) bond interaction. Reproduced with permission from ref. 68. Copyright 2000 American Chemical Society.

This study demonstrates that lower valent titanium (LVT) can activate a B–H bond through σ bond coordination to the borane moiety. This interaction weakens the B–H bond as well as the Ti–B bond and plays a key role in the oxidative addition of B–H bonds in titanium complexes.[66]

3. Dinitrogen coordination and reduction

The efficient utilization of dinitrogen to generate nitrogen-containing molecules remains a challenge in the synthetic community.[69–72] Nitrogen is a major feedstock in the synthesis of ammonia, an ingredient for the production of fertilizers,[73] and N-heterocycles which are important for drug synthesis.[74] The inertness of dinitrogen is a barrier to the catalytic activation of the nitrogen triple bond which has a BDE of about 225 kcal mol^{-1}.[69] The low lying highest occupied molecular orbital (HOMO; 15.6 eV) together with the high energy lowest unoccupied molecular orbital (LUMO; 7.3 eV) disfavor electron transfer and Lewis acid–base reactions. Although the Haber–Bosch process for the industrial production of ammonia utilizes transition metal-based catalysts, nitrogen activation through metal coordination wasn't considered in the reduction until decades after the process was developed.[75]

Interest in dinitrogen coordination to transition metals began when the ruthenium complex, $[Ru(NH_3)_5N_2]^{2+}$, was synthesized demonstrating both coordination and weakening of the N–N triple bond.[75,76] The rationale for the N–N triple bond weakening is based on the electron redistribution between the metal orbitals and the ligand orbitals upon dinitrogen coordination to a metal center.[77–79] When a small molecule like dinitrogen binds to a metal center, a dative bond is formed between a filled non-bonding orbital of the molecule and empty d-orbitals (d_{z^2} or $d_{x^2-y^2}$) of the metal. The metal then back-donates electrons from its filled d-orbitals (d_{xz}, d_{yz}, or d_{xy}) to empty π* orbitals of coordinated nitrogen. This back-donation stabilizes the transition metal–dinitrogen complex and weakens the N–N triple bond. Fig. 7 shows a schematic representation of the back-bonding interaction between a dinitrogen ligand and a metal complex.[78]

Correlation between the N–N bond length and the bond order is often used to estimate the degree of bond activation, with a longer bond length indicative of a greater bond activation. The mode of bonding of the dinitrogen molecule to the metal plays a key role in the extent of bond activation. Generally, there are three bonding modes for dinitrogen to metal centers; mononuclear end-on, dinuclear end-on, and side-on mode (see Fig. 8). In the mononuclear end-on bonding mode, a lesser degree of activation is observed (**8**,[76] **9**[80]) compared to the dinuclear end-on bonding mode (**10**,[81] **11**,[82] **13**[83]). The end-on bonding modes are particularly common among the late transition metals.

In the side-on bonding mode, the filled π-N_2 orbital forms bridging bonds with the metal d-orbitals of σ-symmetry (**12**,[84] **14**[83]). This bonding mode is more prevalent in early metal

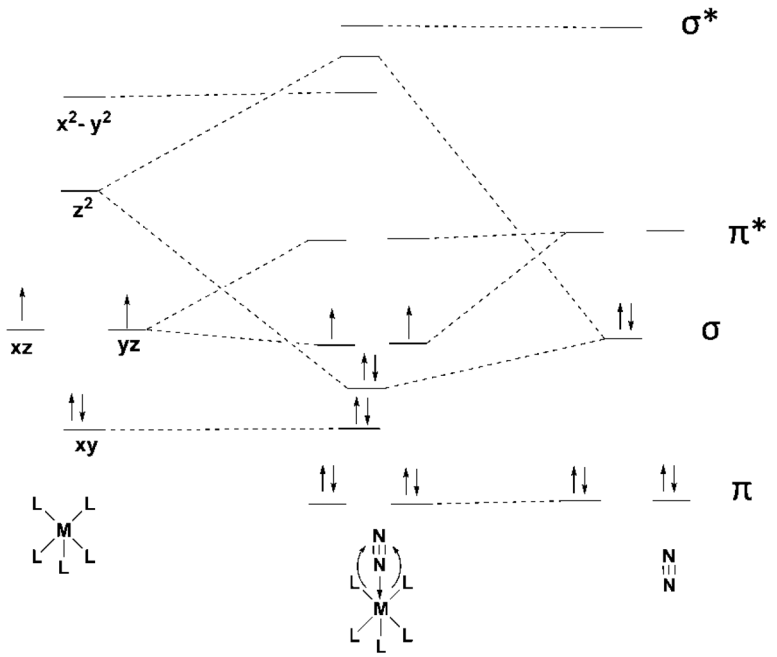

Fig. 7 Molecular orbital diagram showing an interaction between a metal complex (ML_5) and dinitrogen for an $ML_5(\eta^2\text{-}N_2)$ complex. Reproduced with permission from ref. 78. Copyright 1984 Elsevier.

chemistry, and may be due to the lack of an additional d-orbital for back-donation.[69]

An early example of the full characterization of a titanium-side-on bound dinitrogen complex is the work of Pez and co-workers.[85] A tetrametallic titanocene cluster with a $\mu^3,\eta^2,\eta^1,\eta^1$-$N_2$ ligand was synthesized, and the N–N bond length in the cluster was determined to be 1.301 Å (**15**), indicative of a highly activated N–N bond. Other related early studies of dinuclear titanocene dinitrogen complexes such as $[(\eta^5\text{-}C_5H_5)_2Ti(p\text{-}C_6H_4CH_3)]_2(\mu^2\text{-}N_2)$ (**16**) (N–N bond length = 1.162 Å)[86] and $[(\eta^5\text{-}C_5H_5)_2Ti(PMe_3)]_2(\mu^2\text{-}N_2)$ (**17**) (N–N bond length = 1.191 Å)[87] have been reported and have served as the basis for other future studies.[88,89] Bercaw conducted a detailed study on dinitrogen coordination to $(\eta^5\text{-}C_5Me_5)_2Ti$ and reported the existence of three different titanocene-dinitrogen complexes under varying reaction conditions (**18–20**) (see Fig. 9).[90] Complex **18** was the least soluble and was isolated and characterized by X-ray crystallography.[91] The complex was found to consist of two asymmetrical units with N–N bond distances of 1.165 Å and 1.155 Å.

Thorn and Hoffman reported studies on the structure and solid-state magnetic data of complex **18** and established that the π-interaction of the two titanium b_2 orbitals with the N_2 π* orbitals is the dominant component of the Ti–N≡N–Ti bonding, consistent with a "push–pull" interaction where N_2 bridges a π-donor to a π-acceptor metal.[89,92] A similar approach was reported by Berry and coworkers who demonstrated that the treatment of a benzene solution of bis(trimethylphosphine)titanocene, $Cp_2Ti(PMe_3)_2$, with dinitrogen resulted in the formation of a bridging titanocene-dinitrogen complex, $[(\eta^5\text{-}C_5H_5)_2Ti(PMe_3)]_2(\mu^2\text{-}N_2)$ (**17**).[87] The solid-state structure of the complex revealed a relatively long N–N bond (1.191 Å) and short Ti–N bonds which is consistent with a significant back-bonding from the titanium centers to the coordinated dinitrogen (Scheme 11).

The coordinated dinitrogen in complex **17** was found to be quite labile, with the complex forming $Cp_2Ti(CO)_2$ under an atmosphere of carbon monoxide, and generating complex **22** under an atmosphere of N_2 along with a presumed hydrogen liberation from the Cp ligand when left to stand for several days. Another interesting example of a titanocene dinuclear nitrogen complex is the $[(\eta^5\text{-}C_5H_3\text{-}1,3\text{-}(SiMe_3)_2)_2Ti]_2(\mu^2,\eta^1,\eta^1\text{-}N_2)$ complex (**23**) synthesized by Chirik and coworkers.[93]

Under an atmosphere of N_2, $(\eta^5\text{-}C_5H_3\text{-}1,3\text{-}(SiMe_3)_2)_2TiCl$ was reduced with sodium amalgam to generate royal blue crystals of the complex **23** with a weakly activated N–N bond length of 1.164 Å. The presence of the weakly activated N–N bond suggests a weakly coordinated dinitrogen to the titanium center. This weak Ti–N interaction was further explored by reacting **23** with an excess amount of Me_3SiN_3. This resulted in the liberation of 3 equivalents of N_2 with the isolation of the imido complex **24** as red crystals with the complex having a Ti–N bond length of 1.722 Å (see Scheme 13). Imido complexes have been reported as possible intermediates in the reduction of dinitrogen to ammonia.[94,95]

Complex **24** was found to be thermally stable when heated up to 110 °C in benzene for several days and showed high reactivity with dihydrogen, generating the titanocene amido hydride complex **25** (see Scheme 14).[93]

More recently, Chirik and coworkers reported the synthesis and characterization of a trinuclear dinitrogen titanocene complex.[83] Stirring $(\eta^5\text{-}C_5H_3\text{-}1,3\text{-}Me_2)_2TiI$ with excess equiva-

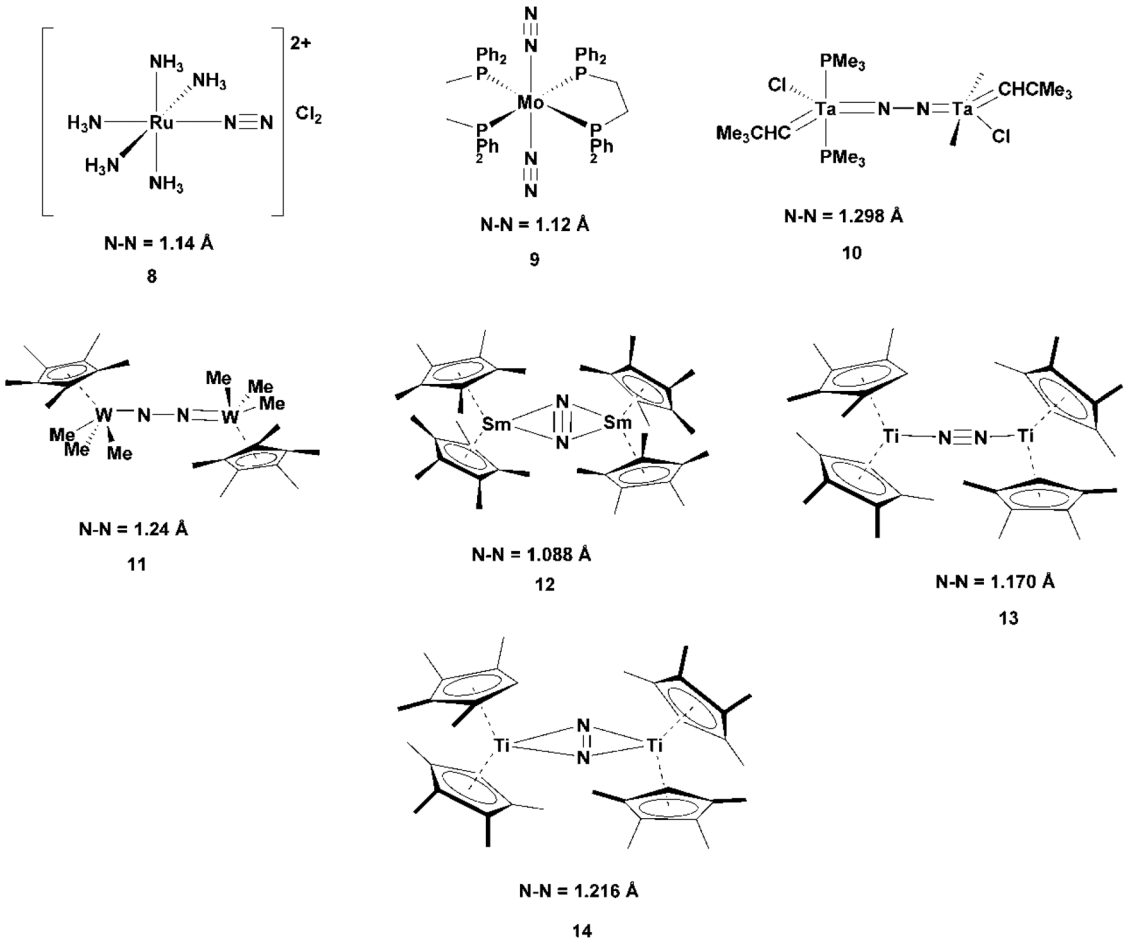

Fig. 8 Bonding modes for dinitrogen to metal centers. Reproduced with permission from ref. 76 and 80–84. Copyright 1988, 1990, 2012, and 1982 American Chemical Society. Copyright 1969 the Royal Society of Chemistry.

lents of KC_8 under a dinitrogen atmosphere for three days, followed by filtration and recrystallization, furnished the complex **26** as blue-green crystals. The N–N bond in trinuclear complex **26**, consistent with either a $[N_2]^{3-}$ or $[N_2]^{4-}$ ligand, has an N–N bond length of 1.320 Å and is the longest observed N–N bond in a titanocene dinitrogen complex (Scheme 15).

Gambarotta and coworkers reported the synthesis and characterization of a non-cyclopentadienyl titanium–dinitrogen complex having a N–N bond distance of 1.289 Å.[96] The reaction of *trans*-$(TMEDA)_2TiCl_2$ (TMEDA = *N*,*N*,*N*′,*N*′-tetramethylethylenediamine) with 1 equivalent of $(Me_3Si)_2NLi$ in toluene under an atmosphere of nitrogen at −80 °C formed a purple jelly suspension which turned into a deep-brown solution upon standing overnight at room temperature. Evaporation and crystallization from ether at −30 °C provided brown crystals of $[(Me_3Si)_2N]TiCl[(TMEDA)]_2(\mu\text{-}N_2)$ (**27**) with an occasional isolation of the monomeric white crystalline $[(Me_2Si)_2N]_2TiCl_2[(TMEDA)_2Li]$ (**28**) (see Scheme 16).

A reaction of *trans*-$(TMEDA)_2TiCl_2$ with 2.5 equivalents of $(Me_3Si)_2NLi$ in the presence of a small excess of TMEDA under the same reaction conditions generated the complex **29** as deep purple/black crystals and complex **28** (resulting from the competitive reaction). The long N–N bond length (1.289 Å) and short Ti–N bond distance (1.762 Å) in complex **27** denotes a substantial back-bonding or electron delocalization of the $Ti_2(\mu\text{-}N_2)$ moiety. Although complex **29** has an N–N bond length of 1.379 Å, which is significantly longer than that of **27**, the longer Ti–N bond length contrasts with that found in **27**. This observation along with the different bonding modes in **29** posed some difficulties in speculating the extent of N–N bond activation.

The coordination of dinitrogen to titanium obviously plays a key role in the reduction of dinitrogen *via* bond activation. The earliest report of ammonia synthesis mediated by a titanium-based compound was by Vol'pin and Shur. A sub-stoichiometric amount of ammonia was formed by passing dinitrogen through the mixture of $(\eta^5\text{-}C_5H_5)_2TiCl_2$ and C_2H_5MgBr in ether at room temperature and atmospheric pressure for 8 h.[21] This pioneering work has set a precedent for the development of various strategies for ammonia synthesis and N–N bond activation mediated by transition metal-based catalysts.[97–99] Some of the strategies mediated by titanium-based complexes are discussed *vide infra*.

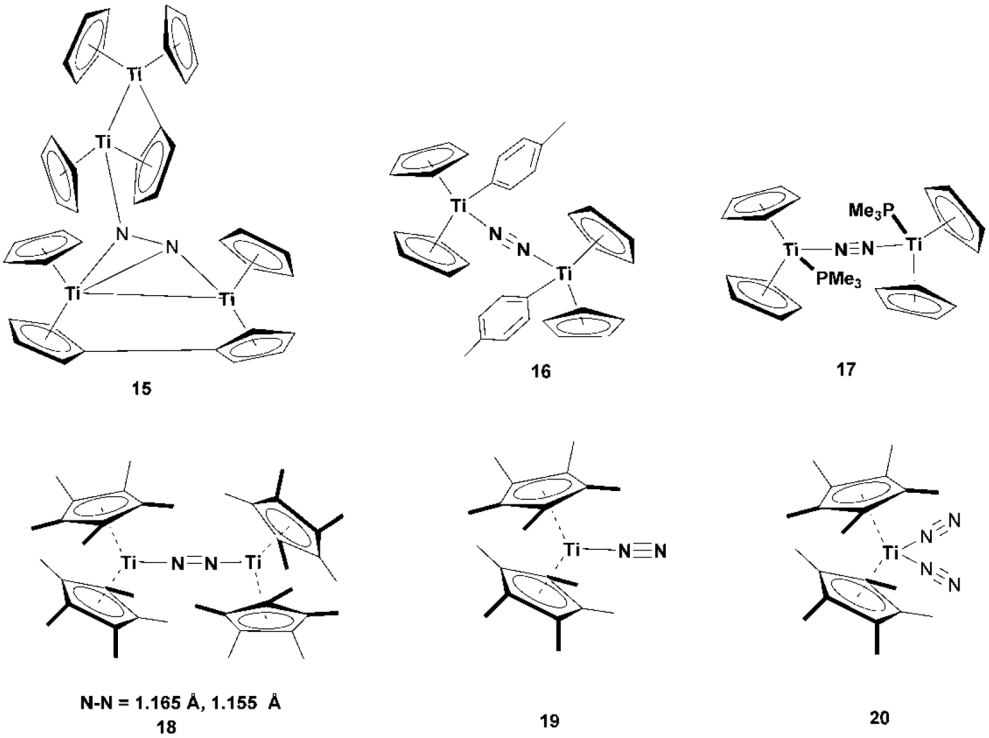

Fig. 9 N–N triple bond activation *via* the formation of Ti–dinitrogen complexes. Reproduced with permission from ref. 85–87 and 90. Copyright 1974, 1982, and 1988 American Chemical Society. Copyright 1979 Elsevier.

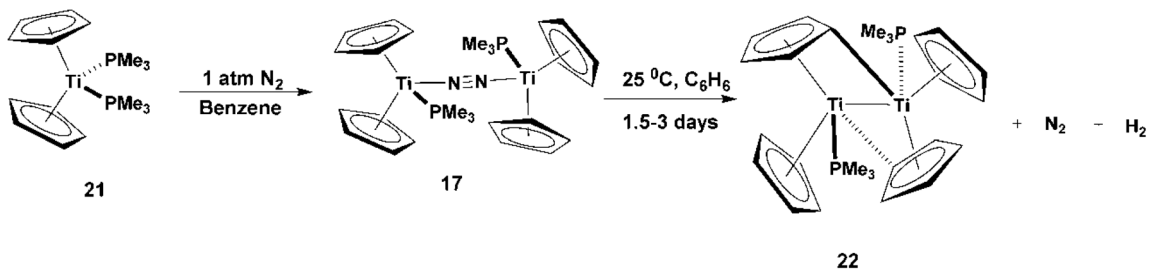

Scheme 11 Synthesis and reactivity of Ti–dinitrogen complex **17**. Reproduced with permission from ref. 87. Copyright 1988 American Chemical Society.

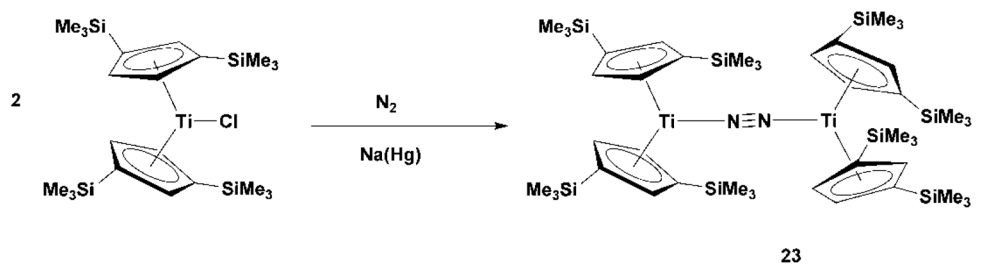

Scheme 12 Synthesis of the titanocene dinuclear nitrogen complex with the activated N–N bond. Reproduced with permission from ref. 93. Copyright 2004 American Chemical Society.

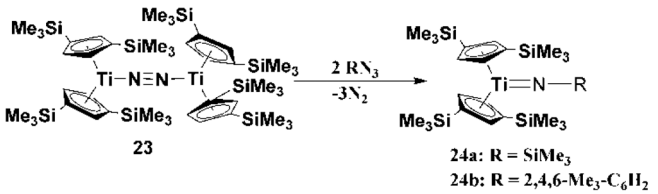

Scheme 13 Formation of the titanocene imido complex (**24**) from the titanocene dinuclear nitrogen complex (**23**). Reproduced with permission from ref. 93. Copyright 2004 American Chemical Society.

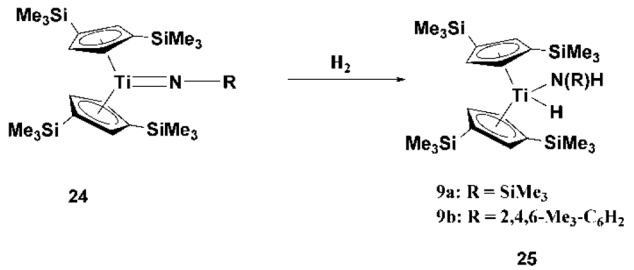

Scheme 14 Reduction of the titanocene imido complex by cleavage of the Ti–N double bond under a hydrogen atmosphere. Reproduced with permission from ref. 92. Copyright 2004 American Chemical Society.

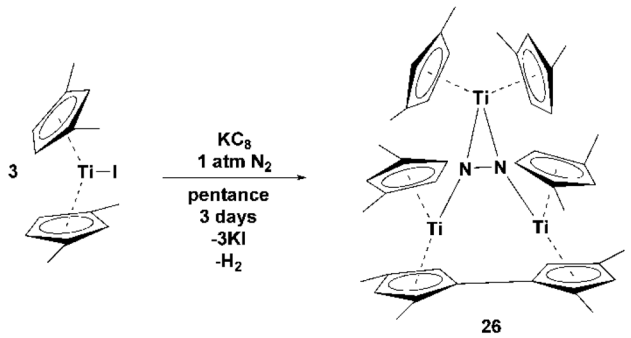

Scheme 15 Synthesis of a trinuclear titanium dinitrogen complex with significant N–N bond activation. Reproduced with permission from ref. 83. Copyright 2012 American Chemical Society.

3.1. Titanium hydrides

The reduction of dinitrogen by transition metal hydrides is very attractive due to the incorporation of both a reducing agent and hydrogen source in one complex and the opportunity to develop homogeneous systems for ammonia synthesis. A review on the use of metal hydrides for dinitrogen hydrogenation was published recently.[100] The discussion below focuses on titanium hydrides. Following the work of Vol'pin and Shur,[21] Brintzinger further investigated the reduction of dinitrogen to ammonia by $(\eta^5\text{-}C_5H_5)_2Ti(Cl)_2$ in the presence of a Grignard reagent.[101,102] Using EPR spectroscopy, it was demonstrated that the hydride species $[(\eta^5\text{-}C_5H_5)_2TiH]_2$ (**30**) was generated after mixing titanocene dichloride, $(\eta^5\text{-}C_5H_5)_2Ti(Cl)_2$, and ethylmagnesium halide (EtMgX) in THF. The titanocene hydride was the only detectable species in the reaction mixture and therefore proposed as the species that coordinated dinitrogen (**31**–**33**). The introduction of a dinitrogen atmosphere in the reaction mixture produces new EPR signals consistent with the complex $[(\eta^5\text{-}C_5H_5)_2TiNH_2]_2$ (**34**) which loses protons from the μ-amino groups upon further addition of the Grignard agent. Treating the final solution with HCl generated the starting material $(\eta^5\text{-}C_5H_5)_2Ti(Cl)_2$ and ammonia (see Scheme 17).

Another notable example of titanium-hydride dinitrogen cleavage is the work of Shima and coworkers.[103] A polyhydride-titanium complex, $\{[(C_5Me_4SiMe_3)Ti]_4(\mu_3\text{-}NH)_2(\mu_2\text{-}H)_4\}$ (**37**), was synthesized by the hydrogenolysis of the titanium alkyl complex $[(C_5Me_4SiMe_3)Ti(CH_2SiMe_3)_3]$ (**36**) under an atmospheric mixture of dihydrogen and dinitrogen in an autoclave. Protonolysis of complex **37** quantitatively generated NH_4Cl. When the titanium alkyl complex **36** was treated with atmospheric dihydrogen under nitrogen-free conditions, the trinuclear titanium-hydride complex $\{[(C_5Me_4SiMe_3)Ti]_3(\mu_3\text{-}H)(\mu_2\text{-}H)_6\}$ (**38**) was formed. The complex **38** was found to be very reactive with dinitrogen and generated the imido/nitrido complex $\{[(C_5Me_4SiMe_3)Ti]_3(\mu_2\text{-}NH)(\mu_3\text{-}N)(\mu_2\text{-}H)_2\}$ (**39**) under a dinitrogen atmosphere. Complex **39** was formed by the reduction of dinitrogen and cleavage of the N–N triple bond. Although the synthesis of ammonia was not achieved in this reaction, this demonstrates a highly activated dinitrogen by the multinuclear titanium complex that resulted in N–N bond cleavage and reduction (Scheme 18).[103,104]

Recently, Hou and coworkers reported the synthesis of a dititanium dihydride framework (**40**) with an N–N bond distance of 1.296 Å, indicating activated dinitrogen.[105] While complex **40** was stable for long periods of time under a N_2 atmosphere at room temperature, heating a hexane or benzene solution of the complex up to 60 °C for 12 h resulted in the cleavage of the N–N bond and the formation of a μ^2-nitrido/μ^2–η^1-phosphinimido dititanium complex. Notably, when a THF solution of the complex was stirred for 6 h, the imido dititanium complex **41** was formed in high yields (see Scheme 19). Water hydrolysis of the imido complex **41** generated NH_3 which was isolated as the ammonium salt upon protonation with HCl in 87% yield.

Leaving a hexane saturated solution of complex **41** to stand at room temperature under an N_2 atmosphere led to the formation of complex **41a** as red crystals with the evolution of hydrogen. Complex **41** was regenerated by exposure to a hydrogen atmosphere, hence, demonstrating their interconversion through dehydrogenation/hydrogenation of the μ^2-imido/μ^2-nitrido units.[105]

3.2. Titanium amides

Hydrogenation of transition metal-amides is another promising approach for the synthesis of ammonia as it serves as an alternative path in overcoming the challenge of nitrogen liberation from coordination to metal centers.[106,107] Chirik reported on the synthesis of free ammonia by catalytic hydrogenolysis of a titanium-amide bond in $(\eta^5\text{-}C_5Me_4SiMe_3)_2Ti(Cl)$

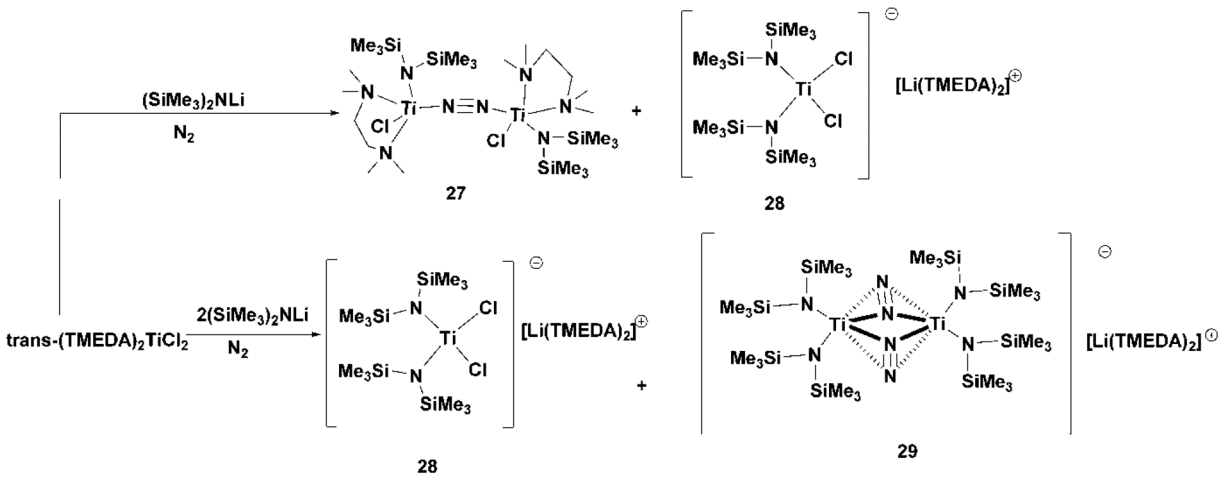

Scheme 16 Complexation of dinitrogen to a non-cyclopentadienyl titanium complex. Reproduced with permission from ref. 96. Copyright 1991 American Chemical Society.

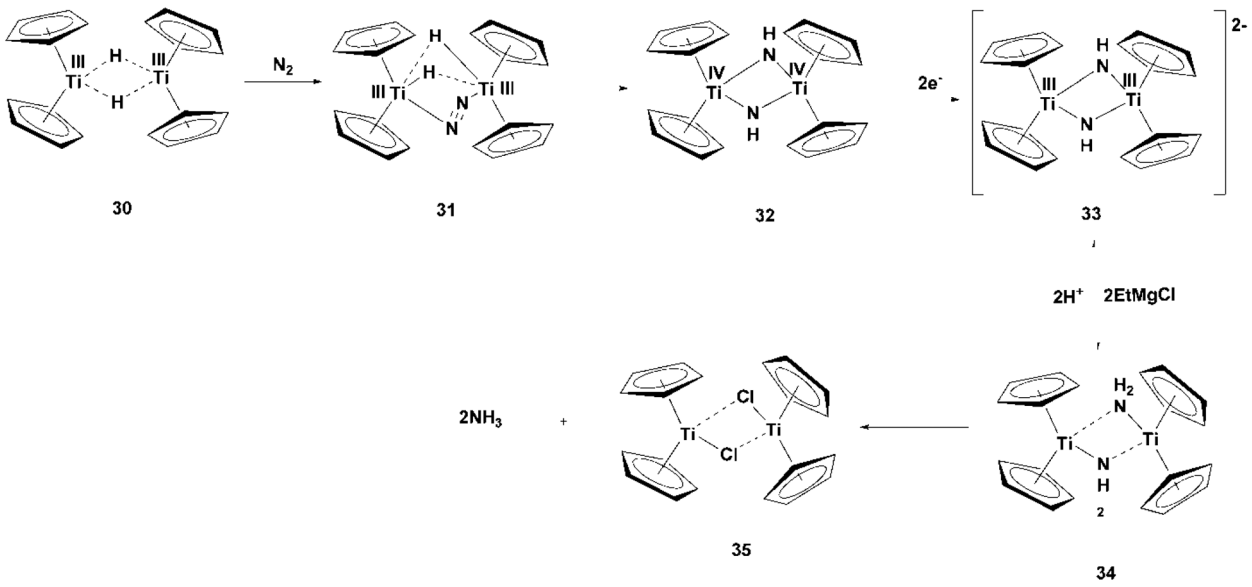

Scheme 17 Dinitrogen coordination to the low-valent titanocene complex and cleavage of the N–N triple bond for ammonia synthesis. Reproduced with permission from ref. 101 and 102. Copyright 1966 American Chemical Society.

NH_2 with a rhodium hydride (**[Rh]–H**), (η^5-C_5Me_5)(py-Ph)RhH (py-Ph = 2-phenylpyridine), serving as the catalyst and promoting N–H bond formation *via* hydrogen atom transfer (see Scheme 20).[108,109] Heating complex **42** with catalytic amounts of **[Rh]–H** in THF for 5 days under an atmosphere of hydrogen produced free ammonia in 92% yield with the recovery of (η^5-$C_5Me_4SiMe_3)_2Ti(Cl)_2$ after treatment of the residue with HCl. The recovery of (η^5-$C_5Me_4SiMe_3)_2Ti(Cl)_2$ indicates that compound **42c** was the only product obtained after the liberation of ammonia. The reaction was optimized by hydrogenating compound **42** with 4 atm of hydrogen gas and 5 mol% of catalytic **[Rh]–H** for a period of 5 days. The low oxidation potential of **[Rh]–H** (−0.38 V *vs.* Fc/Fc^+) relative to that of compound **42** (−2.8 V *vs.* Fc/Fc^+) and the high pK_{ip} of **[Rh]–H** (about 20) compared to that of **42** (15) create a high thermodynamic and kinetic barrier for the catalytic hydrogenation cleavage of the Ti-NH_2 bond to occur *via* initial electron or initial proton transfer. Hence, proton-coupled electron transfer was posited as the likely mechanism of hydrogenolysis.

The pK_{Ip} (ion-pair acidity) of complexes **42** and **43** were determined in 2-methyl-THF by protonating with $HBAr^F_4$ (Ar^F = C_6H_3-3,5-$(CF_3)_2$) and titrating the cationic complexes with pyrrolidine while monitoring spectra changes *via* UV-Vis spectroscopy. Electrochemical studies of the protonated complexes **42a** and **43a** showed irreversible reductions attributed to the dissociation of NH_3. Free ammonia was liberated from both

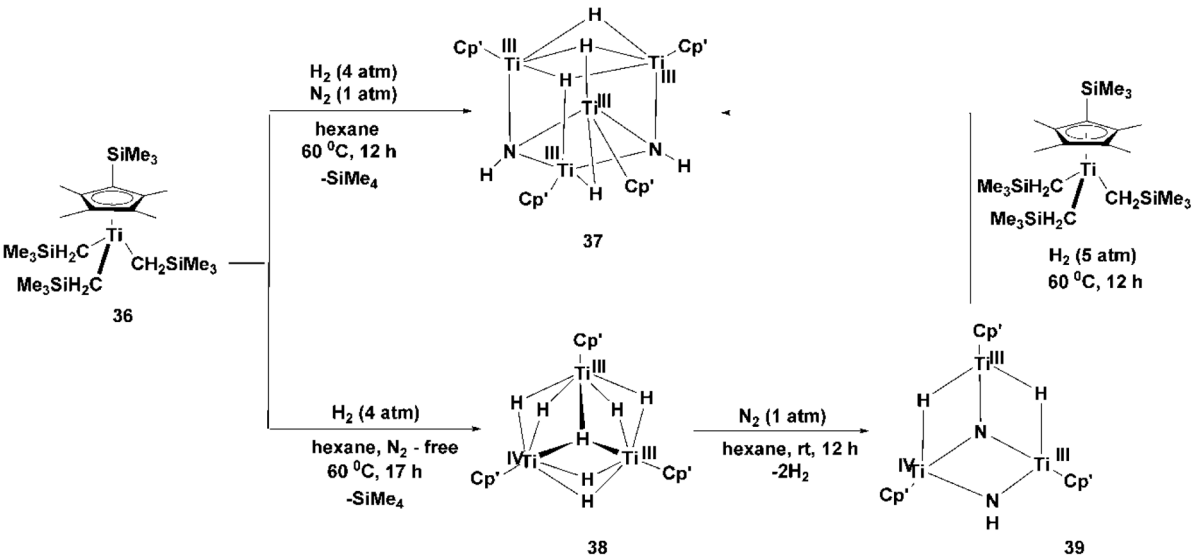

Scheme 18 Titanium-hydride dinitrogen cleavage. Reproduced with permission from ref. 103. Copyright 2013 The American Association for the Advancement of Science.

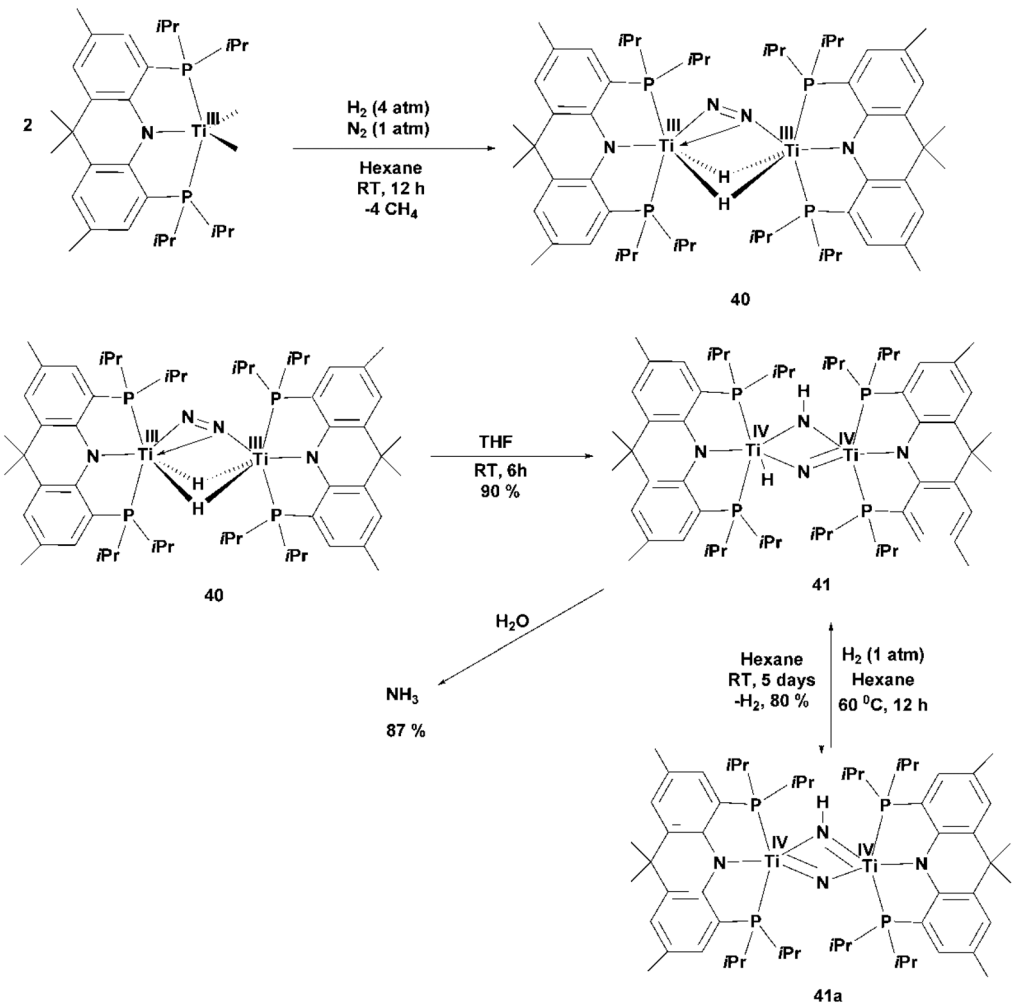

Scheme 19 Dinitrogen cleavage by a dititanium dihydride framework. Reproduced with permission from ref. 105. Copyright 2020 Wiley-VCH Verlag GmbH & Co. KGaA, Weinheim.

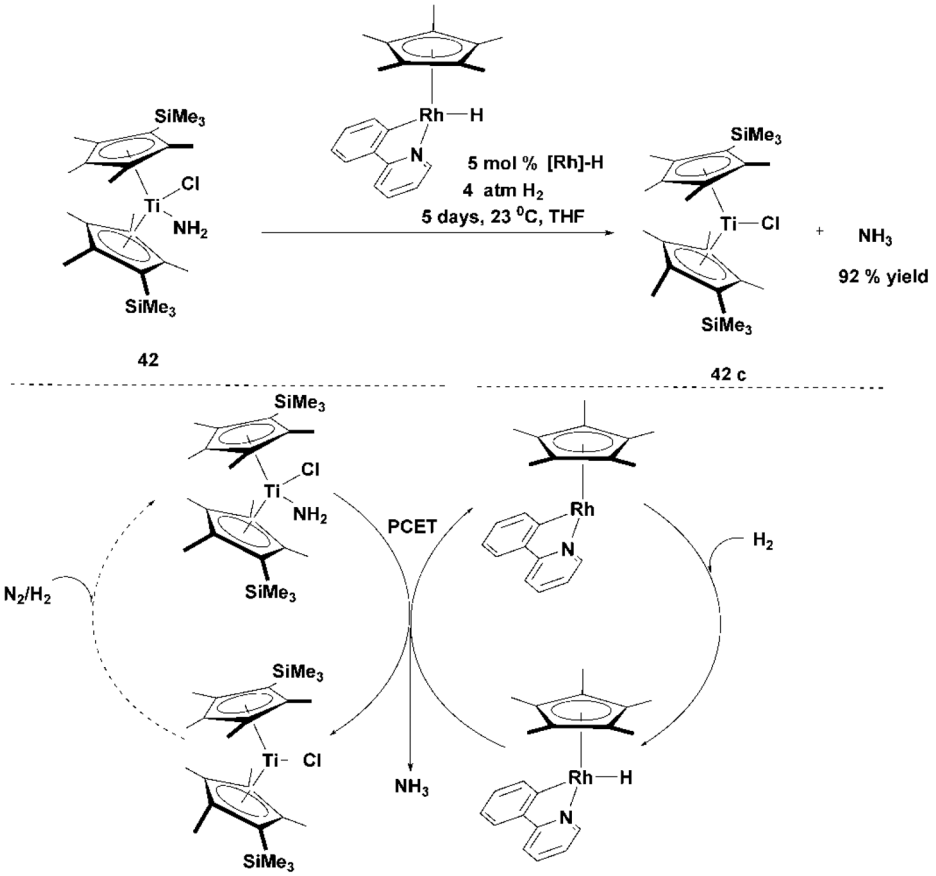

Scheme 20 Catalytic hydrogenolysis of a titanium-amide bond *via* PCET. Reproduced with permission from ref. 109. Copyright 2016 American Chemical Society.

complexes by treatment with Na(Hg) accompanied by the formation of compounds **42c** and **43c** which was confirmed by EPR spectroscopy.

The pK_{IP} and the electrochemical data were used to compute the relative BDFEs using eqn (1) (*vide supra*) (see Table 4). Coordination of ammonia to the metal center results in bond activation of the N–H bond and lowers the BDFE by at least 40 kcal mol^{-1} compared to the BDFE of free ammonia.[31] This induced bond weakening was confirmed by reacting TEMPO (2,2,6,6-tetramethylpiperidine 1-oxyl) with a benzene solution of compounds **42c** or **43c** in the presence of NH_3 gas which resulted in the quantitative formation of TEMPOH (TEMPO-H BDFE in benzene is approximately 65 kcal mol^{-1})[31] and the generation of the compounds **42** and **43** (Scheme 21).

The application of this method was further expanded to include a series of imide-, hydrazide-, and amide-titanocene and zirconocene complexes.[109] A series of transition metal hydrides was chosen as hydrogen atom transfer reagents to assess the thermodynamic parameters and N–H bond forming capabilities of Ti/Zr–nitrogen based compounds. Rhodium hydride (**[Rh]–H**), (η^5-C_5Me_5)(py-Ph)RhH (py-Ph = 2-phenylpyridine),[108] and chromium hydrides, (η^5-C_5H_5)$(CO)_3$CrH (**[Cr]–H**) and (η^5-C_5Me_5) $(CO)_3$CrH (**[Cr]*–H**), were chosen due to their attractive thermochemical properties and demonstrated use in catalytic hydrogenation and radical cyclization reactions (Scheme 22).[110–116]

Repeating the reaction from Scheme 20 with **[Cr]–H** or **[Cr]*–H** produced much lower yields of NH_3 (<40%). Treating complex **45** (see Scheme 22) with catalytic amounts of **[Rh]–H** or **[Cr]–H** in THF for 5 days under an atmosphere of hydrogen generated H_2NNMe_2 with superior reactivity observed in **[Rh]–H** (87% yield) compared to **[Cr]–H** (33%) (see Scheme 22). However, H_2NNMe_2 was not observed when complex **47** was treated with the hydrogenation catalyst, **[Rh]–H**. This difference in reactivity is due to the formation of the more stable (η^5-$C_5Me_4SiMe_3)_2$TiCl (**42c**) from the reaction with complex **45** compared to the generation of the less stable cationic complex $[(\eta^5\text{-}C_5Me_4SiMe_3)_2Ti]^+$ from the reaction with complex **47**. Table 5 shows the structures of hydrogenation catalysts and the titanium complexes with their respective $BDFE_{N-H}$.

Increased reactivity of **[Cr]–H** or **[Cr]*–H** with compound **42** was only observed when stoichiometric amounts were used with yields of NH_3 greater than 90% being obtained. It was detailed that reaction of **[Cr]–H** and **[Cr]*–H** with the titanocene complexes (Scheme 23) leads to the production of the corresponding nitrogen-containing product (NH_3 or NH_2R) and the generation of an organometallic product containing

Table 4 Thermodynamic cycle for the hydrogenolysis of the Ti–N bond and the cleavage of the N–H bond in the titanocene/zirconocene-amide complex. Reproduced with permission from ref. 108. Copyright 2015 American Chemical Society

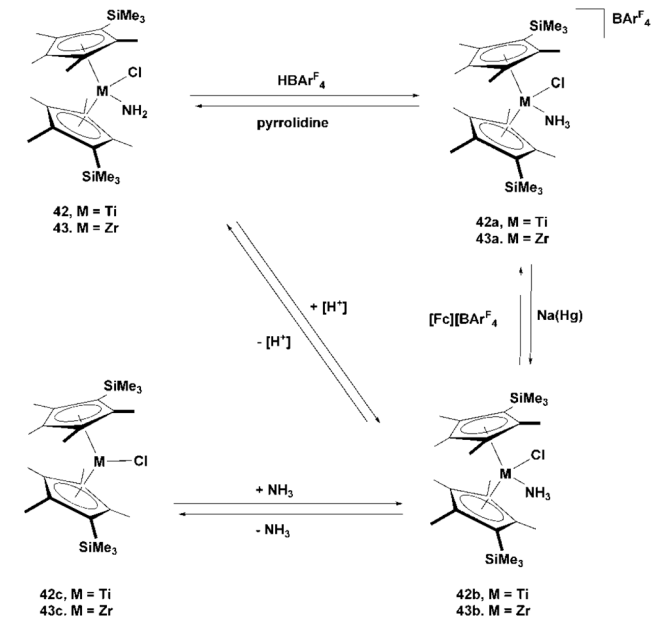

Complex	E_{pc} (V)	pK_{ip}	BDFE$_{N-H}$
42a	−1.60	15.0	61
43a	−2.32	14.7	41

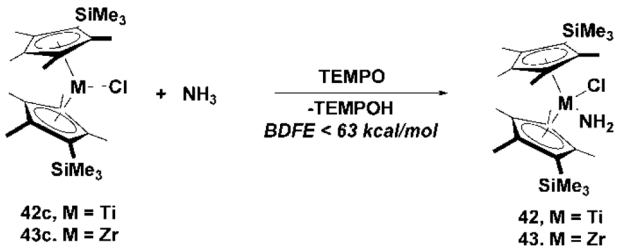

Scheme 21 N–H bond weakening of ammonia induced by coordination to low valent Ti or Zr. Reproduced with permission from ref. 108. Copyright 2015 American Chemical Society.

both the titanocene and chromocene moieties bridged by a carbonyl group (see Table 5).

The ability of **[Cr]–H** and **[Cr]*–H** to react with the Ti(III) complexes where **[Rh]–H** does not react is due to the formation of the **[Ti]-CO-[Cr]** bridging complex (**53**) that avoids the generation of the unstable cationic complex $[(\eta^5\text{-}C_5Me_4SiMe_3)_2Ti]^+$; a bridging structure that is not accessible using **[Rh]–H** as the hydrogenation catalyst (Scheme 23).

3.3. Titanium imides and hydrazides

Transition metal-imido (M = NR) and -hydrazido (M = N-NR) complexes provide another route for nitrogen functionalization towards the synthesis of ammonia or other nitrogen-containing compounds. Titanium-imido complexes have been known for decades and have been used in various transformations including reactions with unsaturated compounds, H–H and S–H bond activations, and CO insertions.[117,118] Seminal reports by Bergman and coworkers described the synthesis of a titanium-imido complex, $(\eta^5\text{-}C_5Me_5)_2TiNPh$ (**54**) and its reactivity towards alkenes and alkynes.[119,120] The complex **54**, which can be synthesized from the reaction of $(\eta^5\text{-}C_5Me_5)_2TiC_2H_4$ and PhN_3, reacts with ethylene and acetylene to generate the azametallacycles $(\eta^5\text{-}C_5Me_5)_2Ti(N(Ph)CH_2CH_2)$ (**55**) and $(\eta^5\text{-}C_5Me_5)_2Ti(N(Ph)CHCH)$ (**56**) (see Scheme 24), respectively. Unlike its reaction with acetylene, the reaction of $(\eta^5\text{-}C_5Me_5)_2TiNPh$ with phenyl- and trimethylsilylacetylene activates the C–H bond of the alkynyl to form anilido–acetylide derivatives (**57**) (see Scheme 24).

Although cleavage of the Ti–N bond was not achieved in this reaction, this demonstrates the azaphilicity of low valent titanium complexes and the high reactivity of the Ti–N bond in the resulting titanium–nitrogen complexes compared to free dinitrogen. A similar approach by Chirik and coworkers described the synthesis of a titanocene-imido complex and the hydrogenation of the Ti–N bond to generate a titanocene amido hydride complex (see Scheme 25). Cleavage of the Ti–N bond was observed when a titanocene-imido complex was reacted with a hydrogenation catalyst (**[Rh]–H**) for 5 days under atmospheric hydrogen. The amine product H_2NSiMe_3 was hydrolyzed to ammonia which was recovered as the ammonium salt in 95% yield.[109]

Although the by-product from the titanocene-imido hydrogenolysis was not reported, the titanocene hydride complex, $(\eta^5\text{-}C_5Me_4SiMe_3)_2TiH_2$ (**59**) was likely generated upon reaction completion. Similar hydride complexes of titanocenes have been reported to be stable and isolable. These hydride complexes can be synthesized from low valent titanocenes in the presence of hydrogen.[121–123]

The reactivity of the titanocene-dinitrogen complex **23** with diazoalkanes was explored and it was reported that the addition of diazodiphenylmethane, Ph_2CN_2, to a pentane solution of **23** yielded the complex $(\eta^5\text{-}C_5H_3\text{-}1,3\text{-}(SiMe_3)_2)_2Ti(N_2CPh_2)$ (**59**) as a dark red solid.[93] Complex **59** was found to exist as two isomers which readily react with carbon monoxide to generate the complex $(\eta^5\text{-}C_5H_3\text{-}1,3\text{-}(SiMe_3)_2)_2Ti(\eta^1\text{-}N_2CPh_2)(CO)$ (**60**). The IR stretching frequency of the CO (2044 cm^{-1}) was observed to be lower than that of a free CO stretching frequency (2143 cm^{-1}) and it was proposed that the CO bond order is reduced due to a π-back-bonding interaction arising from a formal Ti–C double bond of a resonance structure (see Scheme 26). Hydrogenation of either complex **59** or **60** yields the titanium hydride complex $(\eta^5\text{-}C_5H_3\text{-}1,3\text{-}(SiMe_3)_2)_2Ti(NHN{=}CPh_2)H$ (**61**).[93]

3.4. Titanium nitrides

In early work, Volpin and coworkers reported the catalytic reduction of dinitrogen by a mixture of $TiCl_4$, Al, and $AlBr_3$ at >50 °C in the presence and absence of solvent. Ammonia was obtained by hydrolysis with yields proportional to the amount

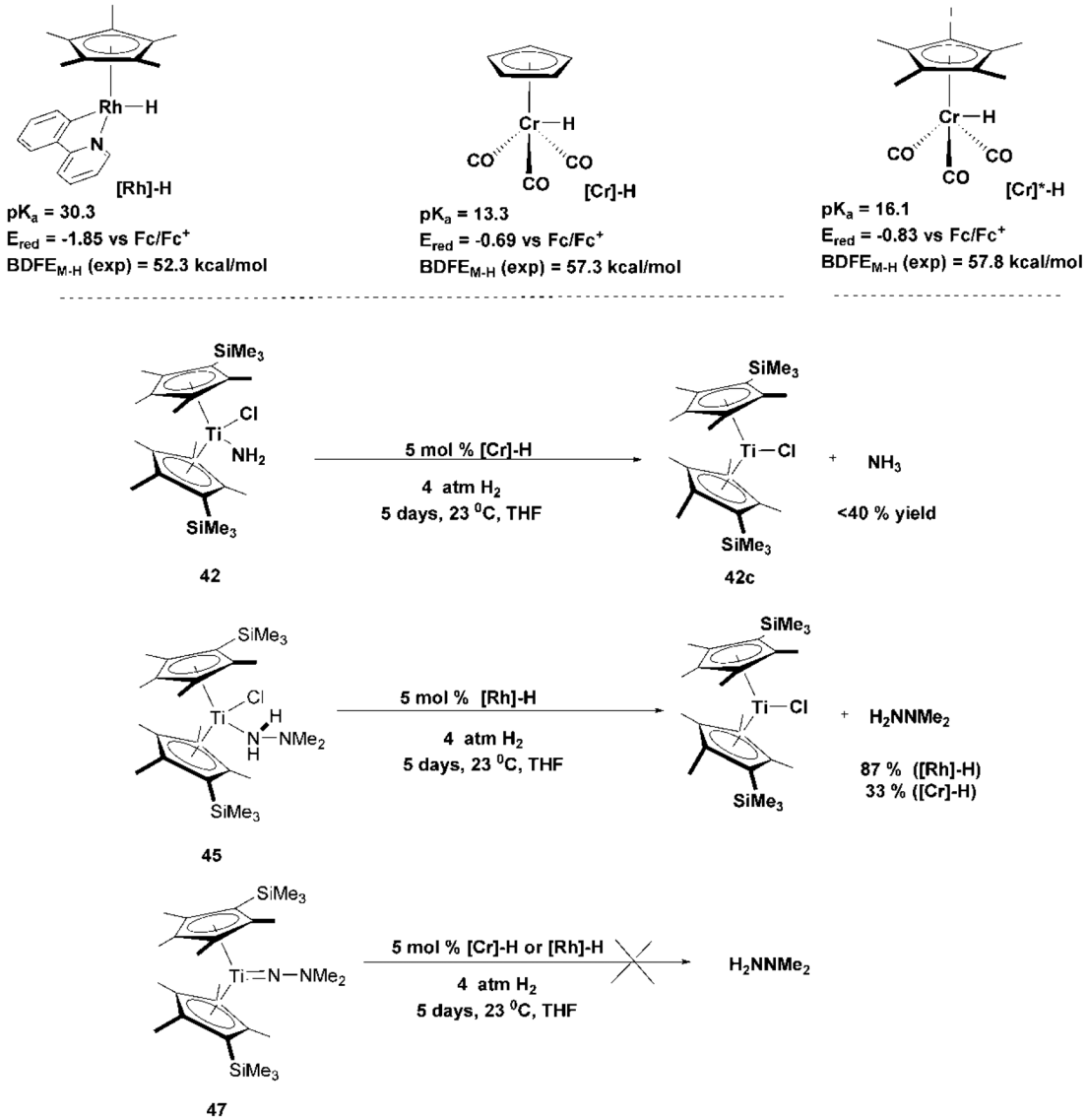

Scheme 22 Reaction of titanocene-nitrogen complexes with hydrogenation catalysts for the cleavage of the Ti–N bond. Reproduced with permission from ref. 109. Copyright 2016 American Chemical Society.

of Al and $AlBr_3$.[107] Heating a benzene solution of $TiCl_4$ in the presence of Al and $AlBr_3$ up to 130 °C at 100 atm generates the low valent titanium(II) compound, $TiCl_2$, which forms the stable complex $(C_6H_6)TiCl_2(AlBr_3)_2$ that acts as the active catalyst for dinitrogen fixation. In the absence of Al and $AlBr_3$ the complex $(C_6H_6)TiCl_2(AlBr_3)_2$ reacts with dinitrogen to form a nitride complex, $(C_6H_6)[(TiCl_2)(AlBr_3)_2]_3N$, which upon hydrolysis, produces a stoichiometric amount of ammonia. Structural information of the various intermediates was not provided by the authors and the chemical composition of the intermediates formed during the reaction is proposed.

The uptake and reduction of dinitrogen by a titanium(II)alkoxide complex that proceeds through a titanium–nitride intermediate was reported by Van Tamelen and coworkers.[124,125] Exposure of the titanium(II)alkoxide (**63**) to atmospheric nitrogen resulted in the reversible coordination of dinitrogen to form a Ti–N_2 complex (**64**) which is reduced to a nitride intermediate by sodium naphthalenide. Hydrogen abstraction from the ethereal solvent used in the reaction by the nitride intermediate generated the ammonia product. The titanium–nitride complex was not fully characterized; however, careful extractions and precipitations gave an unstable air-sensitive powder that was reported to be a nitride complex consisting of titanium, nitrogen, sodium, and isopropoxide units that liberated ammonia on reaction with water or alcohols (Scheme 27).[124]

Substituting the solvent for deuterated THF produced deuterated ammonia albeit in very low yields (10%) compared to the non-deuterated solvent reaction set-up (60–65%). This slow rate and poor yield of ammonia confirm that the hydro-

Table 5 Structures of hydrogenation catalysts and titanium/zirconium–nitrogen complexes with their respective $BDFE_{N-H}$

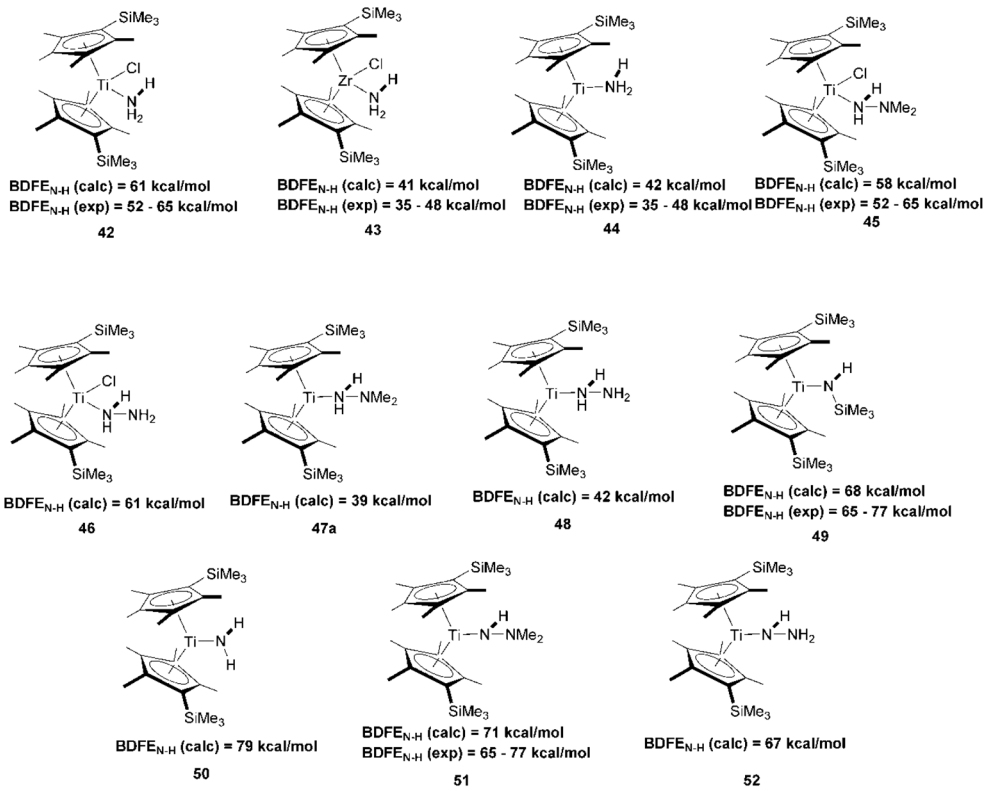

Reproduced with permission from ref (109). Copyright 2016 American Chemical Society.

Reproduced with permission from ref. 109. Copyright 2016 American Chemical Society.

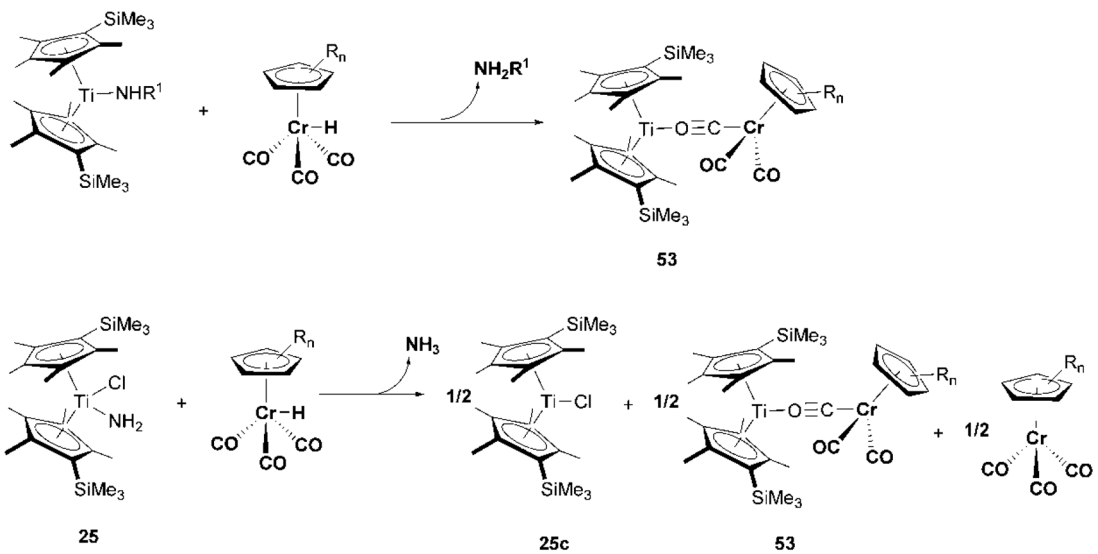

Scheme 23 Formation of a carbonyl-bridging titanocene-chromocene complex in the hydrogenolysis of the Ti–N bond by **[Cr]–H** or **[Cr]*–H**. Reproduced with permission from ref. 109. Copyright 2016 American Chemical Society.

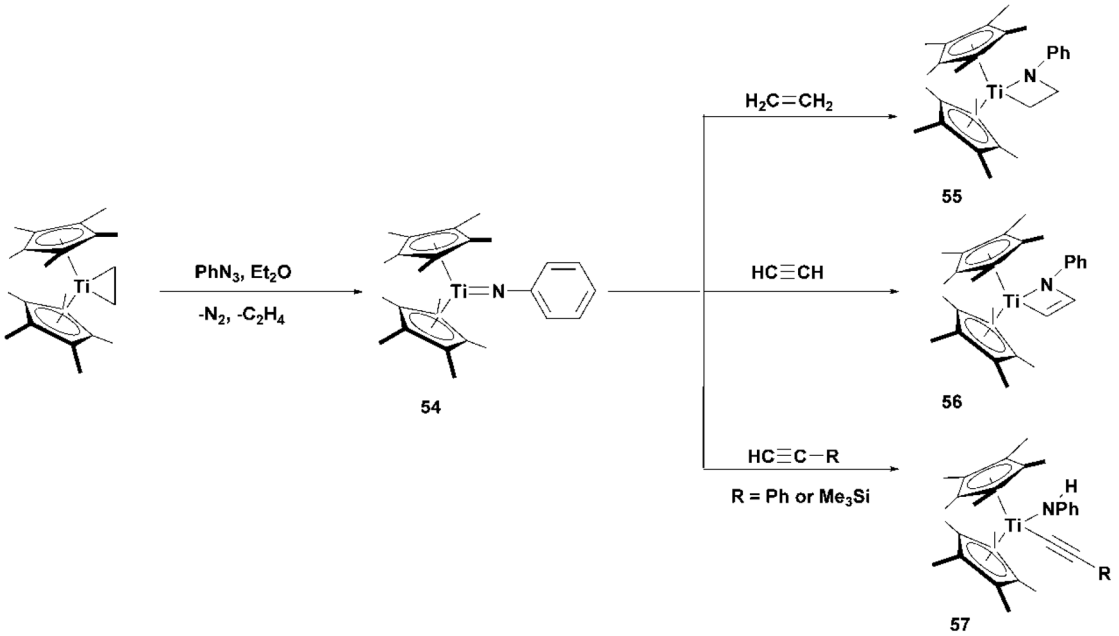

Scheme 24 Reaction of titanocene-imido complex **54** with alkene and alkyne. Reproduced with permission from ref. 119 and 120. Copyright 1998 American Chemical Society and Copyright 1983 American Chemical Society.

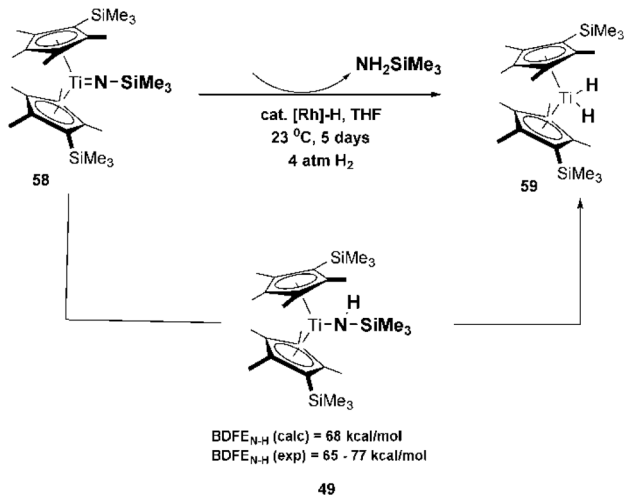

Scheme 25 Hydrogenation of the Ti–N bond of titanocene-imido complex **58** to generate a titanocene amido hydride complex **49**. Reproduced with permission from ref. 109. Copyright 2016 American Chemical Society.

gen abstraction process from the solvent does not contribute to a significant extent to the rapid reduction of the naphthalide.[124]

Liddle and coworkers reported the reductive cleavage of dinitrogen to give a dinitride dititanium dimagnesium ditriamidoamine complex which evolved NH_3 assisted by a phosphine–borane frustrated Lewis pair (FLP).[126] Reduction of [Ti(TrenTMS)Cl] [**65**; TrenTMS$=\{N(CH_2CH_2NSiMe_3)_3\}^{3-}$] with excess KC_8 in the presence of dinitrogen gives [$\{$Ti(TrenTMS)$\}_2(N_2K_2)$] (**66**), which produces up to 18 equivalents of NH_3 when treated with excess H^+/e^-.

Sonification and treatment of **65** with excess Mg in dinitrogen-saturated 1,2-dimethoxyethane (DME) solvent, in the presence of ten equivalents of 1,4-dioxane generates the diamagnetic [$\{$Mg(TrenTMS)$\}_2\{(\mu_3\text{-}N)_2(Ti)_2\}$] (**67**) (see Scheme 28) which produces NH_3 isolated as the ammonium salt.[126,127]

Shima and coworkers described the hydrogenation of a titanium–nitride cluster *via* dihydrogen activation.[128] Heating the tetranuclear complex $[(Cp'Ti)_4(\mu_3\text{-}NH)_2(\mu\text{-}H)_4]$ (Cp′ = $C_5Me_4SiMe_3$) (**68**) at 180 °C for 2 days under a dinitrogen atmosphere resulted in the cleavage of the N–N triple bond and incorporation of the cleaved nitrogens into the tetranuclear cluster to generate the dinitride complex $[(Cp'Ti)_4(\mu_3\text{-}N)_2(\mu_3\text{-}NH)_2]$ (**69**). When a xylene solution of complex **69** was heated at 180 °C for 3 days under atmospheric dihydrogen the complex $(Cp'Ti)_4(\mu_3\text{-}NH)_4$ (**70**) was formed with yields dependent on the pressure of the atmospheric dihydrogen (see Scheme 29). DFT studies of the hydrogenation reaction revealed the coordination of dihydrogen to a titanium center and the migration of the hydrogen atoms to the nitrogen center. Although complete hydrogenolysis to ammonia was not achieved, this reaction demonstrates the facile coordination and cleavage of dinitrogen and dihydrogen at low valent titanium centers which provides a pathway to dinitrogen reduction.

Another interesting example is the reaction of the nitrido complex [$\{Ti(\eta^5\text{-}C_5Me_5)(\mu\text{-}NH)\}_3(\mu_3\text{-}N)$] (**71**) with electrophilic reagents ROTf (R = H, Me; OTf = OSO_2CF_3) to give ammonium salts.[129] Treating a toluene solution of the trinuclear complex **71** with excess triflic acid resulted in the dinuclear complex [$Ti_2(\eta^5$-

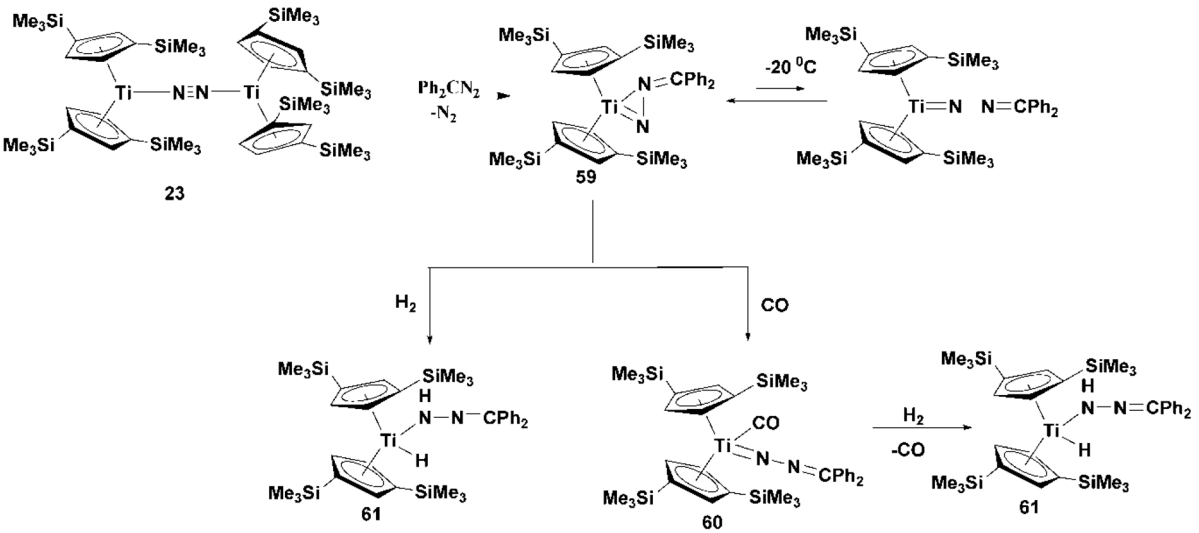

Scheme 26 Reactivity of dinuclear dinitrogen titanium complex **23**. Reproduced with permission from ref. 93. Copyright 2004 American Chemical Society.

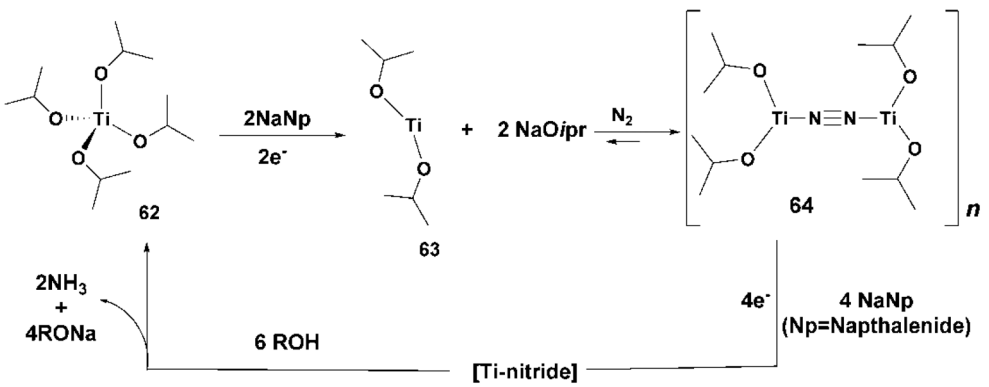

Scheme 27 Uptake and reduction of dinitrogen by a titanium(II)alkoxide complex. Reproduced with permission from ref. 124. Copyright 1969 American Chemical Society.

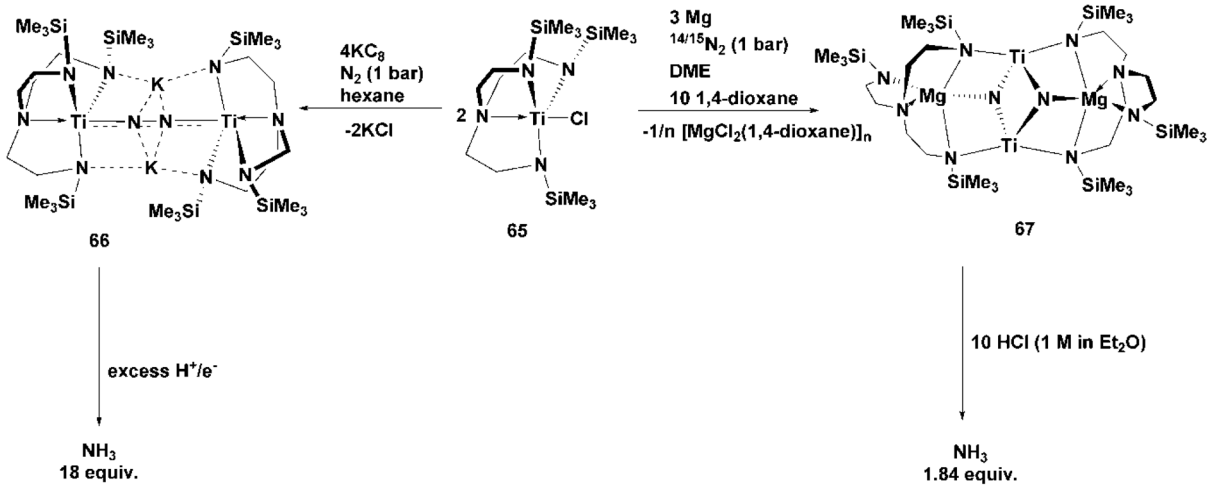

Scheme 28 Reductive cleavage of dinitrogen *via* a dinitride dititanium dimagnesium ditriamidoamine complex. Reproduced with permission from ref. 126. Copyright 2019 Wiley-VCH Verlag GmbH & Co. KGaA, Weinheim.

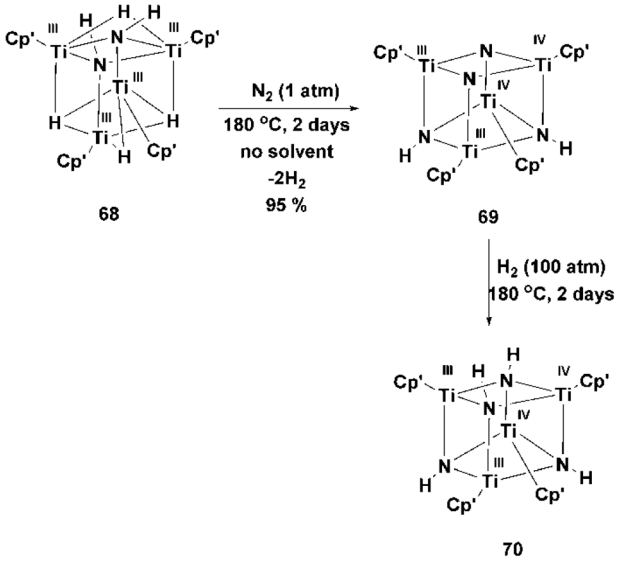

Scheme 29 Hydrogenation of a titanium–nitride cluster *via* dihydrogen activation. Reproduced with permission from ref. 128. Copyright 2019 American Chemical Society.

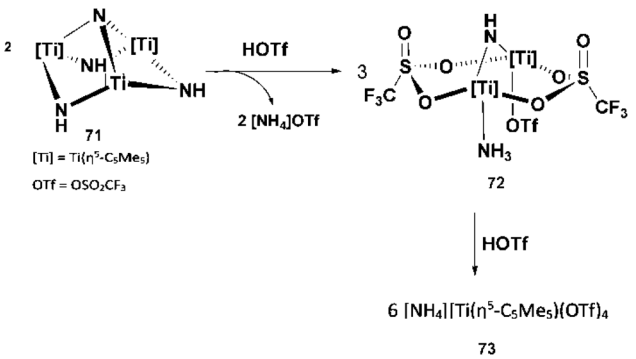

Scheme 30 Reaction of the nitrido complex $[\{Ti(\eta^5\text{-}C_5Me_5)(\mu\text{-}NH)\}_3(\mu_3\text{-}N)]$ (**71**) with electrophilic reagents to give ammonium salts. Reproduced with permission from ref. 129. Copyright 2020 American Chemical Society.

$C_5Me_5)_2(\mu\text{-}N)(NH_3)(\mu\text{-}O_2SOCF_3)_2(OTf)]$ (**72**) and $[NH_4]OTf$ (see Scheme 30). Further treatment of complex **72** with excess MeOTf or HOTf reagents led to the formation of ammonium salts $[NR_4][Ti(\eta^5\text{-}C_5Me_5)(OTf)_4]$ (R = Me (**73**), H (**74**)).

4. Electrocatalysis

Although studies on the use of electrochemistry for ammonia synthesis were reported as early as the 1960s, significant interest in this field accelerated in the past decade.[130–132] The electrochemical route to ammonia synthesis offers several advantages over the Haber–Bosch process. The lower temperature and pressure involved in the electrochemical process as well as the use of water as a source of hydrogen compared to natural gas is very attractive and increases the overall sustainability and economy of the ammonia production process.[131] One of the major challenges in the electrochemical synthesis of ammonia is the competitive reduction of dinitrogen and the evolution of hydrogen gas by electrocatalysts. Designing electrocatalysts with high selectivity for dinitrogen reduction and optimizing electrochemical systems to reduce the hydrogen evolution process will increase the efficiency of electrocatalytic ammonia synthesis.

A notable example of electrocatalytic dinitrogen reduction using a non-cyclopentadienyl ligated titanium compound is demonstrated in the seminal work of van Tamelen and coworkers.[132,133] An electrolysis cell containing 1,2-dimethoxyethane (glyme) solution of titanium tetraisopropoxide, $Ti(O^iPr)_4$, naphthalene, tetrabutylammonium chloride, and aluminum isopropoxide was fitted with an aluminum anode and a nichrome cathode. The solution was stirred for 11 days under an atmosphere of dinitrogen to ensure that the conductance of the cell was significantly reduced. The aluminum anode was completely consumed during the reaction and converted to aluminum nitride (see Scheme 31). Hydrolysis of this solution generated ammonia gas which was converted to an ammonium salt. The yield of NH_3 obtained was 610% per Ti. Titanium tetraisopropoxide was required for the reaction to proceed, however, when naphthalene was removed from the reaction, the yield of NH_3 diminished significantly. This observation demonstrated that the presence of naphthalene was necessary for electron shuttling, being reduced to naphthalide by the nichrome cathode and oxidized back to naphthalene by titanium–nitrogen intermediate. The authors proposed that the aluminum isopropoxide, while also serving as an electrolyte, promoted the release of ammonia from the low valent titanium compound, thereby facilitating the coordination of additional dinitrogen (see Scheme 31).

The first report of the use of $(\eta^5\text{-}C_5H_5)_2TiCl_2$ for electrocatalytic dinitrogen fixation and ammonia synthesis was reported by Becker and coworkers.[134] The reduction of methanolic and THF solutions of $(\eta^5\text{-}C_5H_5)_2TiCl_2$ at either glassy carbon or platinum electrodes in the presence of catechol as a complexation agent under a nitrogen atmosphere, generated ammonia, albeit in very low yields. However, the yield of

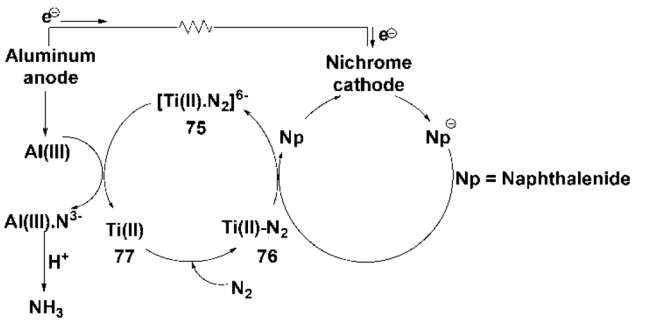

Scheme 31 Electrocatalytic dinitrogen reduction using a non-cyclopentadienyl ligated titanium compound. Reproduced with permission from ref. 133. Copyright 1969 American Chemical Society.

ammonia increased by 400% when a base (MeONa) was introduced and by 200% when the divalent cation (usually Mg^{2+}) was introduced to the solution. It was proposed that in the presence of the base, catechol undergoes deprotonation and forms an intermediate with the reduced Ti complex and that the intermediate (**80**) plays a key role in the reduction of dinitrogen (see Scheme 32).

More recent work by Yoon and coworkers demonstrated the electrocatalytic synthesis of ammonia from nitrogen and proton sources such as wet tetrahydrofuran (THF), methanol and water using titanocene dichloride $(\eta^5\text{-}C_5H_5)_2TiCl_2$ in a two-electrode cell containing 1.0 M LiCl as the electrolyte.[135] The highest rate of ammonia synthesis, 9.5×10^{-10} mol cm^{-2} s^{-1} M per $(\eta^5\text{-}C_5H_5)_2TiCl_2$, was achieved at −1 V in water, and the highest faradaic efficiency (0.95%) was achieved at −2 V in THF. This difference is attributed to the ability of nitrogen to access the active sites on the electrode surface which is a consequence of the different proton concentrations near those sites. DFT calculations were used to estimate the Gibbs free energy of various possible intermediates in the system and a mechanism was proposed as shown below. Electroreduction of the catalyst under a dinitrogen atmosphere generates the titanocene-dinitrogen complex, $(\eta^5\text{-}C_5H_5)_2TiCl\text{-}\mu\text{-}N_2$ (**82**). Electrolysis of H_2O at the electrode surface generates a proton which then migrates to **82**, leading to the intermediate **83**. Successive electron and proton transfers through complexes **84** lead to the release of ammonia (see Scheme 33).

Although complexes **84**, **85**, and **86** were reported to be intermediates in the hydrogenation of dinitrogen, it is likely that titanocene-imido complexes were generated in solution. Imido complexes of titanocene have been reported in titanocene-dinitrogen coordination chemistry to be possible intermediates in dinitrogen reduction.[94,95] Their great stability and highly activated Ti–N bonds make them likely candidates for electrocatalytic dinitrogen hydrogenation (see Scheme 34).

The use of ionic liquids has rapidly gained attention in electrochemistry due to their unique properties such as their

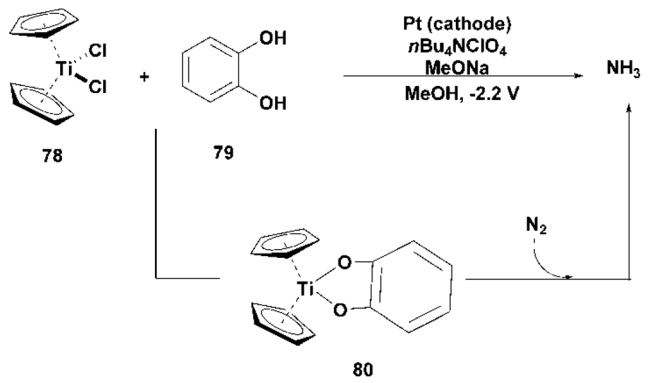

Scheme 32 Titanocene mediated electrocatalytic dinitrogen fixation and ammonia synthesis *via* a Ti-catechol intermediate. Reproduced with permission from ref. 134. Copyright 1987 Elsevier.

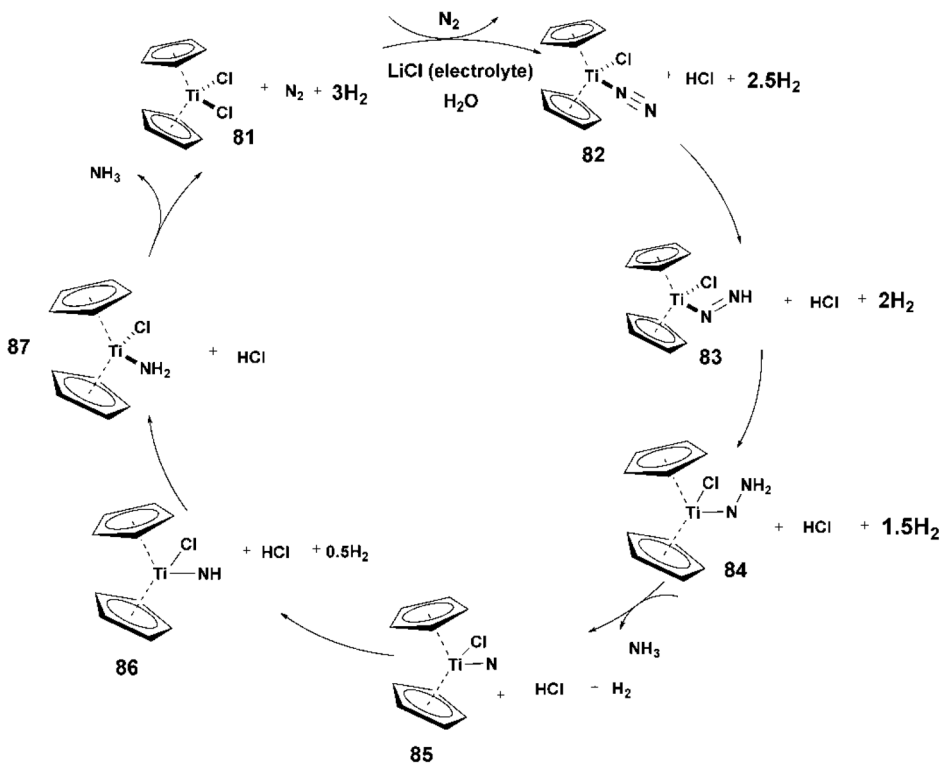

Scheme 33 Electrocatalytic synthesis of ammonia using titanocene. Reproduced with permission from ref. 135. Copyright 2017 American Chemical Society.

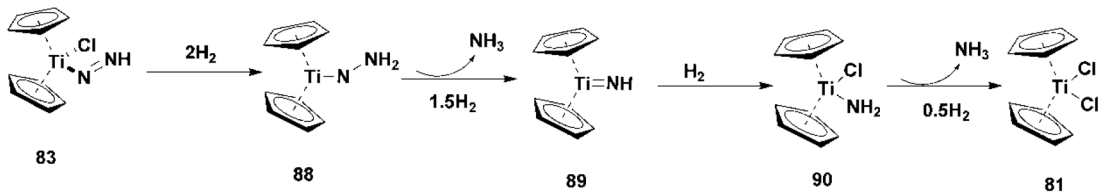

Scheme 34 Possible intermediates in the electrocatalytic dinitrogen hydrogenation reaction.

wide liquid range, low volatility, high conductivity, thermal and chemical stability, and large electrochemical windows.[136,137] Masuda and coworkers reported the electrochemical synthesis of NH_3 from dinitrogen, with water as the proton source, using an ionic liquid and a polymer-supported-$(\eta^5\text{-}C_5H_5)_2TiCl_2$ in a solid polymer electrolyte (SPE) cell under ambient conditions.[138] Butyl-1-methylpyrrolidinium tris (pentafluoroethyl)trifluoro-phosphate, $[C_9H_{20}N]^+$ $[(C_2F_5)_3PF_3]^-$, was chosen as the ionic liquid for the reaction due to its high stability, and was used to fabricate the working electrode. By coating the working electrode with the ionic liquid supported $(\eta^5\text{-}C_5H_5)_2TiCl_2$, a yield of 27% NH_3 per $(\eta^5\text{-}C_5H_5)_2TiCl_2$ was obtained with a current efficiency of 0.2%. The efficiency of this reaction was attributed to the dissociation of chloride from the $(\eta^5\text{-}C_5H_5)_2TiCl_2$ promoted by the electrostatic interaction of the ionic liquid and $(\eta^5\text{-}C_5H_5)_2TiCl_2$.[139] Further studies on the coordination of dinitrogen to $(\eta^5\text{-}C_5H_5)_2TiCl_2$ in a non-coordinating ionic liquid, Pyr_4FAP, by UV-vis/NIR and EPR spectroscopies were carried out. The reduced titanocene was found to be in equilibrium between monomeric $[(\eta^5\text{-}C_5H_5)_2TiCl]$ and dimeric species $[((\eta^5\text{-}C_5H_5)_2TiCl)_2]$ and the EPR spectrum at 77 K revealed the coordination of N_2 to $[(\eta^5\text{-}C_5H_5)_2TiCl]$, confirming that Pyr_4FAP promoted N_2 coordination to the low-valent titanocene.[138] Ammonia was synthesized in an SPE cell using $[((\eta^5\text{-}C_5H_5)_2TiCl)_2]$ in the presence of Pyr_4FAP. The maximum yield of NH_3 obtained per $[((\eta^5\text{-}C_5H_5)_2TiCl)_2]$ was 68% with competitive hydrogen evolution and a maximum current efficiency of 1.44%. The yield and efficiency of the reaction were dependent on the applied charge to the SPE cell. When the coordinating ionic liquid Pyr_4OTf was used, the maximum yield of NH_3 per $[((\eta^5\text{-}C_5H_5)_2TiCl)_2]$ and maximum current efficiency was significantly reduced. This difference in reactivity suggests that a non-coordinating ionic liquid is required to allow for the coordination of dinitrogen to the active titanocene species (see Scheme 35).[138,140]

These studies have shown that titanium complexes can be electrochemically reduced to generate low valent Ti (Ti(II) or Ti (III)) which enables the coordination of dinitrogen. The reduction of the dinitrogen in the Ti-dinitrogen complex is facilitated by the presence of electron shuttling agents and protons from the electrolytic splitting of water to produce ammonia.

5. Outlook and future research

Recent developments in low-valent titanium chemistry present the possibility of exploring untapped and underexplored areas

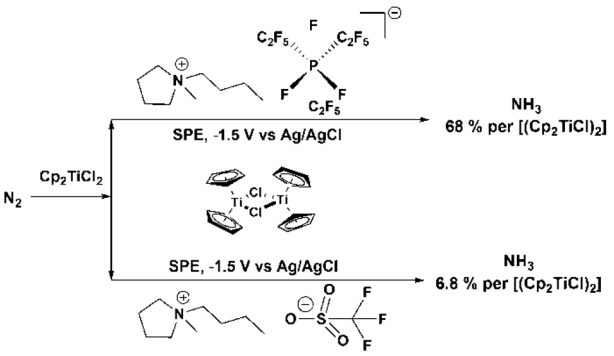

Scheme 35 Electrochemical synthesis of NH_3 from dinitrogen using ionic liquids. Reproduced with permission from ref. 138. Copyright 2017 the Royal Society of Chemistry.

beyond the work described in this review that can potentially expand the synthetic toolbox of small molecule activation. Several promising areas are discussed below.

5.1. Titanium–nitrogen PCET reduction systems

PCET is a redox process that is responsible for electron–proton transfer in many biological systems and has recently been utilized as a process for the design of new platforms for organic reactions. Although this strategy has been applied in various synthetic transformations involving transition metals,[141–143] PCET has only recently been explored in titanium chemistry. The reactivity of titanium complexes in PCET reactions is particularly intriguing, especially with the incorporation of ligands capable of undergoing both protonation and deprotonation processes. The design of ligand environments and precise control of reaction conditions may enable the ability to probe the intricate interplay between electron transfer and proton transfer, resulting in the generation of novel titanium-based species with unique properties.

Balancing the relationship between the pK_a values and the reduction potential of metal complexes is critical for the design of efficient systems minimizing competitive hydrogen gas evolution. Work by Chirik and coworkers described the development of a titanocene amide complex that generated ammonia by a PCET reaction (see Scheme 20 *vide supra*).[108] Additionally, seminal reports from Chirik, Shima, Brintzinger, and their coworkers have demonstrated the ability of low valent Ti to coordinate dinitrogen.[83,93,101–103,105,108] Notably, the work of Chirik and coworkers described the synthesis of a

dinuclear titanium dinitrogen complex **23** through dinitrogen fixation to low valent Ti (*vide supra*).[83,93] The Ti–dinitrogen complex had an activated N–N bond that enabled the hydrogenolysis and the cleavage of the bond to form a titanocene amido hydride complex **25** (see Scheme 12 and Schemes 13, 14). Harnessing the ability of low valent titanium to both coordinate and reduce dinitrogen through PCET has the potential to provide a powerful approach for dinitrogen fixation and reduction.

The reaction in Scheme 36 shows a representative titanocene complex with a pendant substituent capable of undergoing protonation and deprotonation. The low valent titanocene complex has the potential to coordinate a small molecule like dinitrogen and facilitate PCET with the electron being transferred from the Ti and the proton being transferred from the pendant substituent. A seminal example of this approach was introduced by Peters and coworkers who demonstrated that the electrochemical reduction of a cobaltocenium mediator with a pendant amine substituent induces bond weakening of the appended N–H bond to facilitate carbonyl reduction *via* PCET.[144] The ability of low valent Ti to coordinate dinitrogen and induce bond weakening of the N–N bond provides an avenue for the development of an electrochemical titanium-based PCET mediator for dinitrogen reduction. Although the coordination and release of nitrogen ligands in titanium complexes are thermodynamically favorable, there is still a need to overcome the high kinetic barrier that limits the cleavage of Ti–N bonds.

Understanding the thermochemical requirements for the formation of N–H bonds in Ti-coordinated dinitrogen complexes is also necessary in the design of efficient PCET systems for the reduction of dinitrogen. Reviews by Chirik[145] and Peters[146] describe the influence of the intentional combination of reductants and acids of varying strengths in attenuating the overpotential resulting from the formation of N–H bonds. As a consequence, further work directed towards the development of robust titanium-based PCET systems requires a thorough understanding of the BDFEs and mechanisms of bond cleavage of Ti–N and N–N bonds, and the formation of N–H bonds.

5.2. Photocatalytic titanocene-dinitrogen reduction

Although titanocenes have been implicated in cooperative photocatalytic reduction reactions,[147] Gansäuer and Flowers were the first to demonstrate the application of titanocene as a photocatalyst.[12] While the report was focused on epoxide reduction, this strategy can potentially be extended to dinitrogen fixation and reduction. The high affinity of the low valent titanium for nitrogen will enable coordination and reduction of dinitrogen at the titanium metal open site either by an external agent or an appended protonation site on the titanocene complex. Titanium organic frameworks have been reported for the fixation and reduction of dinitrogen to ammonia by visible light photocatalysis,[23,148] however, metal–organic frameworks (MOFs) are generally challenging to synthesize and characterize, particularly Ti-MOFs due to the high reactivity of the Ti-precursors. Titanocenes are relatively straightforward to synthesize, and the cyclopentadienyl ligands can be readily modified for optimal light absorption and reactivity. The scheme below shows a representation of the proposed concept (Scheme 37).

5.3. Tailoring titanium complexes for optimal bond activation

Redox potentials are influenced by ligand substituents on metal complexes and modulate the strength of coordinated ligands. The Bordwell equation (eqn (1)) shows a direct relationship between the redox potential of a complex and the BDFE of coordinated bonds. Previous work by Gansäuer and coworkers demonstrated the addition of substituents on the

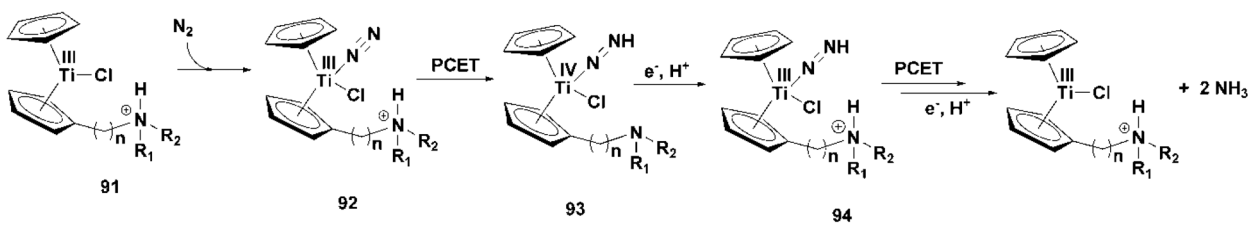

Scheme 36 Proposed design of the titanocene PCET system for cleavage and reduction of dinitrogen.

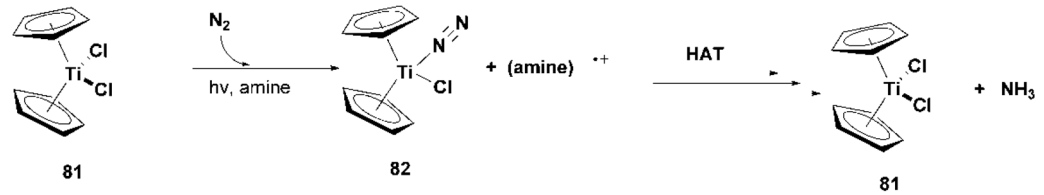

Scheme 37 Proposed design of the photocatalytic titanocene system for cleavage and reduction of dinitrogen.

cyclopentadienyl ligand altered the redox potential by as much as 0.4 V.[149] In related systems, Chirik has shown that the greater the reducing power of the complex, the greater the bond activation of coordinated bonds.[145] As a consequence, the use of appropriate substituents on titanocenes can be used to induce greater activation of coordinated N–N bonds.

6. Summary and conclusions

In this review, the chemistry and reactivity of bond activation by titanium complexes have been outlined. To the best of our knowledge, this is the first report of bond activation with a focus on low-valent titanium. The chemistry of titanium-induced bond weakening highlighted the activation of dinitrogen through electron redistribution between the metal and ligand orbitals in an M → N_2 type interaction and the activation of other small molecules through the thermodynamic consequence of the loss of an H-atom in an M–X–H type interaction. Reports of bond activation of small molecules including water, amides, boranes, and silanes by titanium complexes were critically examined, detailing the extent of bond weakening of the X–H bonds and its role in facilitating challenging organic transformations. The pioneering work on the low-valent titanocene–water system by Cuerva and coworkers[33,34] was described. Additional work on the low-valent titanocene–water system by Gansäuer and coworkers[35] established the intermediates and the role of solvent in attenuating the reactivity of the complex.

An overview of the work of Knowles[43] and Gansäuer[48] and their coworkers on titanocene–amide systems showed that bond weakening of the N–H bond of amides can be affected through the coordination of the amide oxygen to low valent titanocene. Notably, the study of Gansäuer and coworkers demonstrated the duality of the titanocene–amide system which acts as a substrate coordination site as well as a HAT agent. Bond activation of σ Si–H and σ B–H bonds in titanocene–silane and titanocene–borane systems were discussed highlighting works by Ohff, Fan, Scherer, Hartwig and their respective coworkers which further demonstrated the influence of substituents on titanium complexes in inducing bond-weakening.[52,53,62,63,66]

Next, we concentrated on dinitrogen coordination and N–N triple bond activation by low valent titanocene. The modes of bonding of dinitrogen to titanium and the consequence of the bonding modes on the extent of N–N triple bond activation, often indicated by the N–N bond length, were described. Following the discussion on dinitrogen activation, we focused on the reduction of dinitrogen to ammonia by low valent titanium complexes, which was first reported by Vol'pin and Shur in 1966.[21] Titanium based systems such as titanium-hydrides, -amides, -imides, -hydrazides, and -nitrides for the cleavage and reduction of dinitrogen were discussed in detail. Of note among these is the work of Chirik and coworkers on the titanocene–amide system.[108,109] In this report, ammonia was synthesized by cleavage of Ti–N bonds assisted by hydrogenation catalysts. This system allowed for the full experimental and theoretical determination of the $BDFE_{N–H}$ of various amide, imide, and hydrazide complexes of titanocene. Noteworthy is the work of Yoon and coworkers on the electrocatalytic fixation and reduction of dinitrogen to ammonia by titanocene dichloride which demonstrated the ability of nitrogen to access the active sites on the electrode surface, a consequence of the different proton concentrations near those sites.[135]

Overall, this review reveals that low valent titanium complexes can induce weakening in a range of small molecules enabling a range of challenging transformations including the cleavage and reduction of dinitrogen. While progress has been made in designing titanium-based systems for the synthesis of ammonia and other nitrogen-based small molecules, there is still a great deal of work to be done in this area, especially in the development of titanium-based PCET and photocatalytic reductants.

Conflicts of interest

There are no conflicts to declare.

Acknowledgements

We thank the US National Science Foundation (CHE-1954892) for support.

References

1 A. J. Hunt, T. J. Farmer and J. H. Clark, in *Element Recovery and Sustainability*, ed. A. Hunt, The Royal Society of Chemistry, 2013, pp. 1–28.
2 K. S. Egorova and V. P. Ananikov, *Angew. Chem., Int. Ed.*, 2016, **55**, 12150–12162.
3 Z. W. Davis-Gilbert and I. A. Tonks, *Dalton Trans.*, 2017, **46**, 11522–11528.
4 A. Gansäuer, S. Hildebrandt, E. Vogelsang and R. A. Flowers II, *Dalton Trans.*, 2016, **45**, 448–452.
5 T. McCallum, X. Wu and S. Lin, *J. Org. Chem.*, 2019, **84**, 14369–14380.
6 T. Hilche, S. L. Younas, A. Gansäuer and J. Streuff, *ChemCatChem*, 2022, **14**, e202200530.
7 J. E. McMurry, *Chem. Rev.*, 1989, **89**, 1513–1524.
8 A. Gansäuer, H. Bluhm and M. Pierobon, *J. Am. Chem. Soc.*, 1998, **120**, 12849–12859.
9 A. Rosales, J. L. Oller-López, J. Justicia, A. Gansäuer, J. E. Oltra and J. M. Cuerva, *Chem. Commun.*, 2004, 2628–2629.
10 R. E. Estévez, J. L. Oller-López, R. Robles, C. R. Melgarejo, A. Gansäuer, J. M. Cuerva and J. E. Oltra, *Org. Lett.*, 2006, **8**, 5433–5436.
11 S. P. Morcillo, D. Miguel, S. Resa, A. Martín-Lasanta, A. Millán, D. Choquesillo-Lazarte, J. M. García-Ruiz, A. J. Mota, J. Justicia and J. M. Cuerva, *J. Am. Chem. Soc.*, 2014, **136**, 6943–6951.

12 Z. Zhang, T. Hilche, D. Slak, N. R. Rietdijk, U. N. Oloyede, R. A. Flowers and A. Gansäuer, *Angew. Chem., Int. Ed.*, 2020, **59**, 9355–9359.
13 L. E. Aleandri, B. Bogdanovicć, A. Gaidies, D. J. Jones, S. Liao, A. Michalowicz, J. Rozière and A. Schott, *J. Organomet. Chem.*, 1993, **459**, 87–93.
14 O. G. Kulinkovich and A. De Meijere, *Chem. Rev.*, 2000, **100**, 2789–2834.
15 K. A. Keaton and A. J. Phillips, *J. Am. Chem. Soc.*, 2006, **128**, 408–409.
16 G. W. O'Neil and A. J. Phillips, *Tetrahedron Lett.*, 2004, **45**, 4253–4256.
17 Y. Hashimoto, U. Mizuno, H. Matsuoka, T. Miyahara, M. Takakura, M. Yoshimoto, K. Oshima, K. Utimoto and S. Matsubara, *J. Am. Chem. Soc.*, 2001, **123**, 1503–1504.
18 M. Mori, K. Hori, M. Akashi, M. Hori, Y. Sato and M. Nishida, *Angew. Chem., Int. Ed.*, 1998, **37**, 636–637.
19 S. Fortier and A. Gomez-Torres, *Chem. Commun.*, 2021, **57**, 10292–10316.
20 G. Henrici-Olivé and S. Olivé, *Angew. Chem., Int. Ed. Engl.*, 1969, **8**, 650–659.
21 M. E. Vol'pin and V. B. Shur, *Nature*, 1966, **209**, 1236.
22 M. Manßen and L. L. Schafer, *Chem. Soc. Rev.*, 2020, **49**, 6947–6994.
23 J. Zhu, P.-Z. Li, W. Guo, Y. Zhao and R. Zou, *Coord. Chem. Rev.*, 2018, **359**, 80–101.
24 J. M. Arber, D. S. Urch, D. M. P. Mingos and S. J. Royse, *J. Chem. Soc., Chem. Commun.*, 1982, 1241–1243.
25 G. Frenking, in *Modern Coordination Chemistry*, ed. N. Winterton and J. Leigh, Royal Society of Chemistry, Cambridge, 2007, pp. 111–122.
26 R. G. Agarwal, S. C. Coste, B. D. Groff, A. M. Heuer, H. Noh, G. A. Parada, C. F. Wise, E. M. Nichols, J. J. Warren and J. M. Mayer, *Chem. Rev.*, 2022, **122**, 1–49.
27 N. G. Boekell and R. A. Flowers, *Chem. Rev.*, 2022, **122**, 13447–13477.
28 S. Y. Reece, J. M. Hodgkiss, J. Stubbe and D. G. Nocera, *Philos. Trans. R. Soc., B*, 2006, **361**, 1351–1364.
29 E. C. Gentry and R. R. Knowles, *Acc. Chem. Res.*, 2016, **49**, 1546–1556.
30 S. Hammes-Schiffer, *ChemPhysChem*, 2002, **3**, 33–42.
31 J. J. Warren, T. A. Tronic and J. M. Mayer, *Chem. Rev.*, 2010, **110**, 6961–7001.
32 J. M. Mayer, *Annu. Rev. Phys. Chem.*, 2004, **55**, 363–390.
33 A. G. Campaña, R. E. Estévez, N. Fuentes, R. Robles, J. M. Cuerva, E. Buñuel, D. Cárdenas and J. E. Oltra, *Org. Lett.*, 2007, **9**, 2195–2198.
34 M. Paradas, A. G. Campaña, T. Jiménez, R. Robles, J. E. Oltra, E. Buñuel, J. Justicia, D. J. Cárdenas and J. M. Cuerva, *J. Am. Chem. Soc.*, 2010, **132**, 12748–12756.
35 A. Gansäuer, M. Behlendorf, A. Cangönül, C. Kube, J. M. Cuerva, J. Friedrich and M. van Gastel, *Angew. Chem., Int. Ed.*, 2012, **51**, 3266–3270.
36 N. G. Boekell, C. O. Bartulovich, S. Maity and R. A. Flowers, *Inorg. Chem.*, 2023, **62**, 5040–5045.
37 D. Dakternieks, D. J. Henry and C. H. Schiesser, *J. Chem. Soc., Perkin Trans. 2*, 1997, 1665–1670.
38 W. R. Dolbier and X. X. Rong, *J. Fluor. Chem.*, 1995, **72**, 235–240.
39 L. M. Brines, M. K. Coggins, P. C. Y. Poon, S. Toledo, W. Kaminsky, M. L. Kirk and J. A. Kovacs, *J. Am. Chem. Soc.*, 2015, **137**, 2253–2264.
40 R. Sahoo, S. C. Pal and M. C. Das, *ACS Energy Lett.*, 2022, **7**, 4490–4500.
41 C. O. Bartulovich and R. A. Flowers, *Dalton Trans.*, 2019, **48**, 16142–16147.
42 K. T. Tarantino, D. C. Miller, T. A. Callon and R. R. Knowles, *J. Am. Chem. Soc.*, 2015, **137**, 6440–6443.
43 L. Q. Nguyen and R. R. Knowles, *ACS Catal.*, 2016, **6**, 2894–2903.
44 F. G. Bordwell, S. Zhang, X.-M. Zhang and W.-Z. Liu, *J. Am. Chem. Soc.*, 1995, **117**, 7092–7096.
45 K.-W. Huang and R. M. Waymouth, *J. Am. Chem. Soc.*, 2002, **124**, 8200–8201.
46 M. K. Mahanthappa, K.-W. Huang, A. P. Cole and R. M. Waymouth, *Chem. Commun.*, 2002, 502–503.
47 K.-W. Huang, J. H. Han, A. P. Cole, C. B. Musgrave and R. M. Waymouth, *J. Am. Chem. Soc.*, 2005, **127**, 3807–3816.
48 Y.-Q. Zhang, V. Jakoby, K. Stainer, A. Schmer, S. Klare, M. Bauer, S. Grimme, J. M. Cuerva and A. Gansäuer, *Angew. Chem., Int. Ed.*, 2016, **55**, 1523–1526.
49 J. A. Osborn, F. H. Jardine, J. F. Young and G. Wilkinson, *J. Chem. Soc. A*, 1966, 1711.
50 R. H. Crabtree, H. Felkin and G. E. Morris, *J. Organomet. Chem.*, 1977, **141**, 205–215.
51 M.-F. Fan and Z. Lin, *Organometallics*, 1999, **18**, 286–289.
52 M.-F. Fan, G. Jia and Z. Lin, *J. Am. Chem. Soc.*, 1996, **118**, 9915–9921.
53 A. Ohff, P. Kosse, W. Baumann, A. Tillack, R. Kempe, H. Goerls, V. V. Burlakov and U. Rosenthal, *J. Am. Chem. Soc.*, 1995, **117**, 10399–10400.
54 R. H. Crabtree, *Angew. Chem., Int. Ed. Engl.*, 1993, **32**, 789–805.
55 Z. Lin, *Chem. Soc. Rev.*, 2002, **31**, 239–245.
56 S. A. Cohen and J. E. Bercaw, *Organometallics*, 1985, **4**, 1006–1014.
57 B. Demerseman, R. Mahé and P. H. Dixneuf, *J. Chem. Soc., Chem. Commun.*, 1984, 1394–1396.
58 V. V. Burlakov, A. V. Polyakov, A. I. Yanovsky, Yu. T. Struchkov, V. B. Shur, M. E. Vol'pin, U. Rosenthal and H. Görls, *J. Organomet. Chem.*, 1994, **476**, 197–206.
59 U. Rosenthal, A. Ohff, W. Baumann, R. Kempe, A. Tillack and V. V. Burlakov, *Organometallics*, 1994, **13**, 2903–2906.
60 E. Spaltenstein, P. Palma, K. A. Kreutzer, C. A. Willoughby, W. M. Davis and S. L. Buchwald, *J. Am. Chem. Soc.*, 1994, **116**, 10308–10309.
61 U. Schubert, in *Advances in Organometallic Chemistry*, Elsevier, 1990, vol. 30, pp. 151–187.
62 M.-F. Fan and Z. Lin, *Organometallics*, 1997, **16**, 494–496.
63 W. Scherer, P. Meixner, K. Batke, J. E. Barquera-Lozada, K. Ruhland, A. Fischer, G. Eickerling and K. Eichele, *Angew. Chem., Int. Ed.*, 2016, **55**, 11673–11677.

64 P. Meixner, K. Batke, A. Fischer, D. Schmitz, G. Eickerling, M. Kalter, K. Ruhland, K. Eichele, J. E. Barquera-Lozada, N. P. M. Casati, F. Montisci, P. Macchi and W. Scherer, *J. Phys. Chem. A*, 2017, **121**, 7219–7235.
65 W. Scherer, P. Meixner, J. E. Barquera-Lozada, C. Hauf, A. Obenhuber, A. Brück, D. J. Wolstenholme, K. Ruhland, D. Leusser and D. Stalke, *Angew. Chem., Int. Ed.*, 2013, **52**, 6092–6096.
66 J. F. Hartwig, C. N. Muhoro, X. He, O. Eisenstein, R. Bosque and F. Maseras, *J. Am. Chem. Soc.*, 1996, **118**, 10936–10937.
67 C. N. Muhoro, X. He and J. F. Hartwig, *J. Am. Chem. Soc.*, 1999, **121**, 5033–5046.
68 W. H. Lam and Z. Lin, *Organometallics*, 2000, **19**, 2625–2628.
69 M. P. Shaver and M. D. Fryzuk, *Adv. Synth. Catal.*, 2003, **345**, 1061–1076.
70 M. Hidai and Y. Mizobe, *Pure Appl. Chem.*, 2001, **73**, 261–263.
71 A. A. Mohamed, *Coord. Chem. Rev.*, 2010, **254**, 1918–1947.
72 R. A. Flowers, *Nat. Synth.*, 2023, **2**, 597–599.
73 J. K. Ladha, H. Pathak, T. J. Krupnik, J. Six and C. Van Kessel, in *Advances in Agronomy*, Elsevier, 2005, vol. 87, pp. 85–156.
74 M. M. Heravi and V. Zadsirjan, *RSC Adv.*, 2020, **10**, 44247–44311.
75 A. D. Allen and C. V. Senoff, *Chem. Commun. (London)*, 1965, 621.
76 C. V. Senoff, *J. Chem. Educ.*, 1990, **67**, 368.
77 G. J. Kubas, *J. Organomet. Chem.*, 2001, **635**, 37–68.
78 P. Pelikán and R. Boča, *Coord. Chem. Rev.*, 1984, **55**, 55–112.
79 T. Yang, Z. Li, X. Wang and G. Hou, *ChemPhysChem*, 2023, **24**, e202200835.
80 M. Hidai, K. Tominari, Y. Uchida and A. Misono, *J. Chem. Soc., Chem. Commun.*, 1969, 1392.
81 S. M. Rocklage, H. W. Turner, J. D. Fellmann and R. R. Schrock, *Organometallics*, 1982, **1**, 703–707.
82 M. B. O'Regan, A. H. Liu, W. C. Finch, R. R. Schrock and W. M. Davis, *J. Am. Chem. Soc.*, 1990, **112**, 4331–4338.
83 S. P. Semproni, C. Milsmann and P. J. Chirik, *Organometallics*, 2012, **31**, 3672–3682.
84 W. J. Evans, T. A. Ulibarri and J. W. Ziller, *J. Am. Chem. Soc.*, 1988, **110**, 6877–6879.
85 G. P. Pez, P. Apgar and R. K. Crissey, *J. Am. Chem. Soc.*, 1982, **104**, 482–490.
86 J. D. Zeinstra, J. H. Teuben and F. Jellinek, *J. Organomet. Chem.*, 1979, **170**, 39–50.
87 D. H. Berry, L. J. Procopio and P. J. Carroll, *Organometallics*, 1988, **7**, 570–572.
88 P. Sobota, B. Jeżowska-Trzebiatowska and Z. Janas, *J. Organomet. Chem.*, 1976, **118**, 253–258.
89 P. J. Chirik, *Organometallics*, 2010, **29**, 1500–1517.
90 J. E. Bercaw, *J. Am. Chem. Soc.*, 1974, 5087.
91 R. D. Sanner, D. M. Duggan, T. C. McKenzie, R. E. Marsh and J. E. Bercaw, *J. Am. Chem. Soc.*, 1976, **98**, 8358–8365.
92 R. Hoffman, M. M.-L. Chen and D. L. Thorn, *Inorg. Chem.*, 1977, **16**, 503.
93 T. E. Hanna, I. Keresztes, E. Lobkovsky, W. H. Bernskoetter and P. J. Chirik, *Organometallics*, 2004, **23**, 3448–3458.
94 S. M. Mullins, A. P. Duncan, R. G. Bergman and J. Arnold, *Inorg. Chem.*, 2001, **40**, 6952–6963.
95 J. A. Pool, E. Lobkovsky and P. J. Chirik, *Nature*, 2004, **427**, 527–530.
96 R. Duchateau, S. Gambarotta, N. Beydoun and C. Bensimon, *J. Am. Chem. Soc.*, 1991, **113**, 8986–8988.
97 Y. Tanabe and Y. Nishibayashi, *Coord. Chem. Rev.*, 2013, **257**, 2551–2564.
98 Y. Tanabe and Y. Nishibayashi, *Chem. Soc. Rev.*, 2021, **50**, 5201–5242.
99 M. J. Chalkley, M. W. Drover and J. C. Peters, *Chem. Rev.*, 2020, **120**, 5582–5636.
100 J. Ballmann, R. F. Munhá and M. D. Fryzuk, *Chem. Commun.*, 2010, **46**, 1013.
101 H. Brintzinger, *J. Am. Chem. Soc.*, 1966, **88**, 4305–4307.
102 H. Brintzinger, *J. Am. Chem. Soc.*, 1966, **88**, 4307–4308.
103 T. Shima, S. Hu, G. Luo, X. Kang, Y. Luo and Z. Hou, *Science*, 2013, **340**, 1549–1552.
104 T. Shima and Z. Hou, in *Nitrogen Fixation*, ed. Y. Nishibayashi, Springer International Publishing, Cham, 2017, vol. 60, pp. 23–43.
105 Z. Mo, T. Shima and Z. Hou, *Angew. Chem., Int. Ed.*, 2020, **59**, 8635–8644.
106 Y. Tanabe and Y. Nishibayashi, *Coord. Chem. Rev.*, 2022, **472**, 214783.
107 M. E. Volpin, M. A. Ilatovskaya, L. V. Kosyakova and V. B. Shur, *Chem. Commun. (London)*, 1968, 1074.
108 I. Pappas and P. J. Chirik, *J. Am. Chem. Soc.*, 2015, **137**, 3498–3501.
109 I. Pappas and P. J. Chirik, *J. Am. Chem. Soc.*, 2016, **138**, 13379–13389.
110 E. O. Fischer and R. L. Pruett, in *Inorganic Syntheses*, ed. J. Kleinberg, John Wiley & Sons, Inc., Hoboken, NJ, USA, 2007, pp. 136–139.
111 D. P. Estes, J. R. Norton, S. Jockusch and W. Sattler, *J. Am. Chem. Soc.*, 2012, **134**, 15512–15518.
112 D. M. Smith, M. E. Pulling and J. R. Norton, *J. Am. Chem. Soc.*, 2007, **129**, 770–771.
113 L. Tang, E. T. Papish, G. P. Abramo, J. R. Norton, M.-H. Baik, R. A. Friesner and A. Rappé, *J. Am. Chem. Soc.*, 2003, **125**, 10093–10102.
114 A. Miyake and H. Kondo, *Angew. Chem., Int. Ed. Engl.*, 1968, **7**, 631–632.
115 T. J. Jaeger and M. C. Baird, *Organometallics*, 1988, **7**, 2074–2076.
116 P. Leoni, A. Landi and M. Pasquali, *J. Organomet. Chem.*, 1987, **321**, 365–369.
117 N. Hazari and P. Mountford, *Acc. Chem. Res.*, 2005, **38**, 839–849.
118 A. E. Guiducci, C. L. Boyd and P. Mountford, *Organometallics*, 2006, **25**, 1167–1187.

119 J. L. Polse, R. A. Andersen and R. G. Bergman, *J. Am. Chem. Soc.*, 1998, **120**, 13405–13414.
120 S. A. Cohen, P. R. Auburn and J. E. Bercaw, *J. Am. Chem. Soc.*, 1983, **105**, 1136–1143.
121 H. Brintzinger and R. H. Marvich, *J. Am. Chem. Soc.*, 1971, **93**, 2046–2048.
122 H. Brintzinger and J. E. Bercaw, *J. Am. Chem. Soc.*, 1970, **92**, 6182–6185.
123 J. Pinkas, R. Gyepes, I. Císařová, J. Kubišta, M. Horáček and K. Mach, *Dalton Trans.*, 2017, **46**, 8229–8244.
124 E. E. Van Tamelen, R. B. Fechter, S. W. Schneller, G. Boche, R. H. Greeley and B. Akermark, *J. Am. Chem. Soc.*, 1969, **91**, 1551–1552.
125 E. E. Van Tamelen, G. Boche, S. W. Ela and R. B. Fechter, *J. Am. Chem. Soc.*, 1967, **89**, 5707–5708.
126 L. R. Doyle, A. J. Wooles and S. T. Liddle, *Angew. Chem., Int. Ed.*, 2019, **58**, 6674–6677.
127 L. R. Doyle, A. J. Wooles, L. C. Jenkins, F. Tuna, E. J. L. McInnes and S. T. Liddle, *Angew. Chem., Int. Ed.*, 2018, **57**, 6314–6318.
128 T. Shima, G. Luo, S. Hu, Y. Luo and Z. Hou, *J. Am. Chem. Soc.*, 2019, **141**, 2713–2720.
129 P. Barriopedro, J. Caballo, M. Mena, A. Pérez-Redondo and C. Yélamos, *Inorg. Chem.*, 2020, **59**, 7631–7643.
130 L. F. Greenlee, J. N. Renner and S. L. Foster, *ACS Catal.*, 2018, **8**, 7820–7827.
131 G. Qing, R. Ghazfar, S. T. Jackowski, F. Habibzadeh, M. M. Ashtiani, C.-P. Chen, M. R. Smith and T. W. Hamann, *Chem. Rev.*, 2020, **120**, 5437–5516.
132 E. E. Van Tamelen and B. Akermark, *J. Am. Chem. Soc.*, 1968, **90**, 4492–4493.
133 E. E. Van Tamelen and D. A. Seeley, *J. Am. Chem. Soc.*, 1969, **91**, 5194–5194.
134 J. Y. Becker, S. Avraham (Tsarfaty) and B. Posin, *J. Electroanal. Chem. Interfacial Electrochem.*, 1987, **230**, 143–153.
135 E.-Y. Jeong, C.-Y. Yoo, C. H. Jung, J. H. Park, Y. C. Park, J.-N. Kim, S.-G. Oh, Y. Woo and H. C. Yoon, *ACS Sustainable Chem. Eng.*, 2017, **5**, 9662–9666.
136 M. Armand, F. Endres, D. R. MacFarlane, H. Ohno and B. Scrosati, *Nat. Mater.*, 2009, **8**, 621–629.
137 P. Hapiot and C. Lagrost, *Chem. Rev.*, 2008, **108**, 2238–2264.
138 A. Katayama, T. Inomata, T. Ozawa and H. Masuda, *Dalton Trans.*, 2017, **46**, 7668–7671.
139 A. Katayama, T. Inomata, T. Ozawa and H. Masuda, *Electrochem. Commun.*, 2016, **67**, 6–10.
140 A. Katayama, T. Inomata, T. Ozawa and H. Masuda, *ChemElectroChem*, 2017, **4**, 3053–3060.
141 O. S. Wenger, *Chem. – Eur. J.*, 2011, **17**, 11692–11702.
142 C. A. Gaggioli, J. Sauer and L. Gagliardi, *J. Am. Chem. Soc.*, 2019, **141**, 14603–14611.
143 T. Kojima, *Bull. Chem. Soc. Jpn.*, 2020, **93**, 1571–1582.
144 M. J. Chalkley, P. Garrido-Barros and J. C. Peters, *Science*, 2020, **369**, 850–854.
145 M. J. Bezdek, I. Pappas and P. J. Chirik, in *Nitrogen Fixation*, ed. Y. Nishibayashi, Springer International Publishing, Cham, 2017, vol. 60, pp. 1–21.
146 M. J. Chalkley and J. C. Peters, *Eur. J. Inorg. Chem.*, 2020, **2020**, 1353–1357.
147 A. Gualandi, F. Calogero, M. Mazzarini, S. Guazzi, A. Fermi, G. Bergamini and P. G. Cozzi, *ACS Catal.*, 2020, **10**, 3857–3863.
148 H. Huang, X.-S. Wang, D. Philo, F. Ichihara, H. Song, Y. Li, D. Li, T. Qiu, S. Wang and J. Ye, *Appl. Catal., B*, 2020, **267**, 118686.
149 A. Gansäuer, C. Kube, K. Daasbjerg, R. Sure, S. Grimme, G. D. Fianu, D. V. Sadasivam and R. A. Flowers, *J. Am. Chem. Soc.*, 2014, **136**, 1663–1671.